ICOS maintains the T follicular helper cell phenotype by down-regulating Krüppel-like factor 2

Jan P. Weber,[1,4]* Franziska Fuhrmann,[1,4]* Randi K. Feist,[1,4]* Annette Lahmann,[1,4]* Maysun S. Al Baz,[1,4] Lea-Jean Gentz,[1,4] Dana Vu Van,[1,4] Hans W. Mages,[4] Claudia Haftmann,[2] René Riedel,[2] Joachim R. Grün,[3] Wolfgang Schuh,[5] Richard A. Kroczek,[4] Andreas Radbruch,[2] Mir-Farzin Mashreghi,[2] and Andreas Hutloff[1,4]

[1]Chronic Immune Reactions, [2]Cell Biology, and [3]Bioinformatics, German Rheumatism Research Centre, a Leibniz Institute, 10117 Berlin, Germany
[4]Molecular Immunology, Robert Koch Institute, 13353 Berlin, Germany
[5]Division of Molecular Immunology, University of Erlangen-Nürnberg, 91054 Erlangen, Germany

The co-stimulators ICOS (inducible T cell co-stimulator) and CD28 are both important for T follicular helper (TFH) cells, yet their individual contributions are unclear. Here, we show that each molecule plays an exclusive role at different stages of TFH cell development. While CD28 regulated early expression of the master transcription factor Bcl-6, ICOS co-stimulation was essential to maintain the phenotype by regulating the novel TFH transcription factor Klf2 via Foxo1. Klf2 directly binds to Cxcr5, Ccr7, Psgl-1, and S1pr1, and low levels of Klf2 were essential to maintain this typical TFH homing receptor pattern. Blocking ICOS resulted in relocation of fully developed TFH cells back to the T cell zone and reversion of their phenotype to non-TFH effector cells, which ultimately resulted in breakdown of the germinal center response. Our study describes for the first time the exclusive role of ICOS and its downstream signaling in the maintenance of TFH cells by controlling their anatomical localization in the B cell follicle.

CORRESPONDENCE
Andreas Hutloff:
hutloff@drfz.de

Abbreviations used: ChIP, chromatin immunoprecipitation; GC, germinal center; geoMFI, geometric mean fluorescence intensity; ICOS, inducible T cell co-stimulator; ICOS-L, ICOS ligand; Klf2, Krüppel-like factor 2; NP, nitrophenol; PNA, peanut agglutinin; PSGL-1, P-selectin glycoprotein ligand-1; S1PR1, sphingosine-1-phosphate receptor 1; TFH, T follicular helper.

T follicular helper (TFH) cells are the $CD4^+$ T cell subset providing help for B cells during the germinal center (GC) reaction (Crotty, 2011; Tellier and Nutt, 2013). They are the prerequisite for the generation of high-affinity memory B cells and long-lived plasma cells. Therefore, manipulation of the TFH response is of particular clinical interest to either promote the generation of protective antibodies during vaccination or to eliminate harmful antibodies in autoimmune diseases or allergy (Craft, 2012; Tangye et al., 2013).

The generation of TFH cells is a multistep process. Two early key events are the up-regulation of the master transcription factor Bcl-6 and the chemokine receptor CXCR5, which results in migration to the border of the T and B cell zone in secondary lymphoid organs. Here, first contact with antigen-specific B cells occurs which seems to be critical for determination of the TFH phenotype and further migration deeper into the B cell follicle, where they provide B cell help by means of high expression of CD40L and production of the cytokines IL-4 and IL-21 (Crotty, 2011; McHeyzer-Williams et al., 2012). In contrast to other effector T cell subsets, TFH memory cells lose their prototypic markers when the GC reaction terminates (Weber et al., 2012). The induction of the TFH phenotype is now relatively well defined, whereas factors that maintain the phenotype of already differentiated TFH cells and the ongoing GC response are still unknown, although this effector phase is of upmost importance from a clinical point of view.

*J.P. Weber, F. Fuhrmann, R.K. Feist, and A. Lahmann contributed equally to this paper.

The Rockefeller University Press $30.00
J. Exp. Med. 2015 Vol. 212 No. 2 217–233
www.jem.org/cgi/doi/10.1084/jem.20141432

The Journal of Experimental Medicine

The blockade of T cell co-stimulatory pathways has emerged as a promising tool for the treatment of autoimmune diseases (Yao et al., 2013). The two closely related co-stimulators CD28 and inducible T cell co-stimulator (ICOS) are both known to be important for T cell–dependent B cell responses. If appropriate co-stimulation is lacking, mice develop very small GCs and have strongly reduced numbers of TFH cells (Walker et al., 1999; McAdam et al., 2001; Tafuri et al., 2001; Akiba et al., 2005; Linterman et al., 2009; Platt et al., 2010). A similar picture can be observed in ICOS-deficient patients, who present with the clinical phenotype of common variable immunodeficiency (Grimbacher et al., 2003; Bossaller et al., 2006). However, the molecular mechanisms behind how ICOS and CD28 influence TFH cells are still not fully understood.

Blockade of the CD28 pathway using a CTLA-4–Ig fusion protein (Abatacept; Brystol-Myers-Squibb) is already in clinical use for the treatment of rheumatoid arthritis (Yao et al., 2013). Recently, a blocking monoclonal antibody against ICOS-L (AMG 557; Amgen) has been successfully tested in a phase Ib study with systemic lupus erythematosus patients and is currently also evaluated for the treatment of lupus arthritis (Sullivan, B.A., W. Tsuji, A. Kivitz, M. Weisman, D.J. Wallace, M. Boyce, M. Mackay, R.J. Looney, S. Cohen, M.A. Andrew, et al. 2013. American College of Rheumatology/Association of Rheumatology Health Professionals Annual Meeting).

In the present study, we reveal unique contributions of the co-stimulatory molecules CD28 and ICOS for different phases of TFH cell development. We show that ICOS, unlike CD28, is not important for early events in TFH cell differentiation like up-regulation of Bcl-6 but for the maintenance of already differentiated TFH cells in the late GC reaction. We identified the transcription factor Krüppel-like factor 2 (Klf2) as a downstream target of ICOS and a novel negative regulator of TFH cell maintenance. Klf2 is repressed by ICOS via the Foxo1 pathway and controls the expression of TFH cell homing markers independently of Bcl-6 by direct binding to regulatory regions of their DNA. Once ICOS signaling is interrupted in a GC reaction, TFH cells leave the B cell zone and subsequently revert their phenotype to non-TFH effector cells. Therefore, we propose as a new concept that the anatomical localization of TFH cells in the B cell follicle determines their fate.

RESULTS

CD28 but not ICOS regulates early key events of TFH differentiation

To analyze the role of CD28 and ICOS co-stimulation for different phases of TFH cell development and the GC reaction, we used an adoptive transfer mouse model with antigen-specific T and B cells from ovalbumin-specific OT-II T cell receptor transgenic and nitrophenol (NP)-specific B1-8i B cell receptor knock-in mice, respectively. Transgenic WT, KO, and recipient's T cells within the same animal could be discriminated in flow cytometry by differential expression of congenic markers (Fig. 1 A). The double transfer of WT and KO T cells allowed for normal differentiation of GC B cells in the recipient and therefore to analyze the T cell–intrinsic effect of the respective co-stimulator deficiency. 8 d after immunization with an NP-OVA conjugate, lack of CD28 or ICOS co-stimulation resulted in a 100-fold or 25-fold reduction in the numbers of TFH cells, respectively (Fig. 1 B).

To understand the molecular mechanisms, we first quantified the expression of key molecules for TFH cell development and function at an early point in time. 3 d after immunization (similar data were obtained for days 2 and 4; not depicted), only a small fraction of CD28-deficient T cells expressed the TFH master transcription factor Bcl-6 (Fig. 2 A). Unexpectedly, we found that ICOS KO T cells up-regulated Bcl-6 to a similar extent as WT T cells, which seems to be in contrast to published data (Choi et al., 2011), as discussed below. In CD28- and ICOS-deficient T cells, the regulation of the two major TFH homing chemokine receptors was significantly impaired with an incomplete down-regulation of CCR7 and reduced up-regulation of CXCR5 (Fig. 2 A). However, when we analyzed the migration of developing TFH cells by immunohistology, ICOS-deficient T cells migrated to a similar extent as WT T cells toward the T/B cell border (Fig. 2 D). In stark contrast, CD28-deficient T cells remained equally distributed in the T cell zone. In the WT group, some T cells had already moved deeper into the B cell zone. These cells were reduced by 50% in the ICOS KO group (unpublished data), which is in line with findings by Xu et al. (2013), demonstrating that at later times (beyond day 4), a substantial difference regarding follicular localization of ICOS-deficient T cells develops.

For molecules that are important for B cell help, a strong difference was seen between CD28- and ICOS-deficient T cells (Fig. 2 B). CD28 KO T cells had only minimal expression of CD40L and were not able to produce significant amounts of IL-4 and IL-21, whereas ICOS KO T cells expressed these factors similarly to their WT counterparts. We also analyzed additional transcription factors that are known to be important for early TFH cell differentiation. *Ascl2*, which was recently identified as a second factor, in addition to Bcl-6, for up-regulation of CXCR5 (Liu et al., 2014), was expressed even more highly in ICOS and CD28 KO T cells (Fig. 2 C). Expression of *c-Maf* was essentially unchanged, whereas *Prdm1* (encoding Blimp-1) was reduced to 50% only in CD28 KO T cells. *Tbx21* (encoding T-bet) was reduced in ICOS and CD28 KO T cells whereas *Gata3* was substantially reduced in CD28 KO T cells, only.

These results show that lack of CD28 co-stimulation prevents up-regulation of all major Th subset master transcription factors, including Bcl-6 and all subsequent TFH differentiation steps. In contrast, ICOS-deficient T cells only show a reduced up-regulation of CXCR5, which is independent of Bcl-6 and Ascl2 expression.

Interruption of ICOS signaling leads to a rapid loss of the TFH phenotype

The aforementioned findings indicate that ICOS might have a specific role for later events of TFH cell development. We

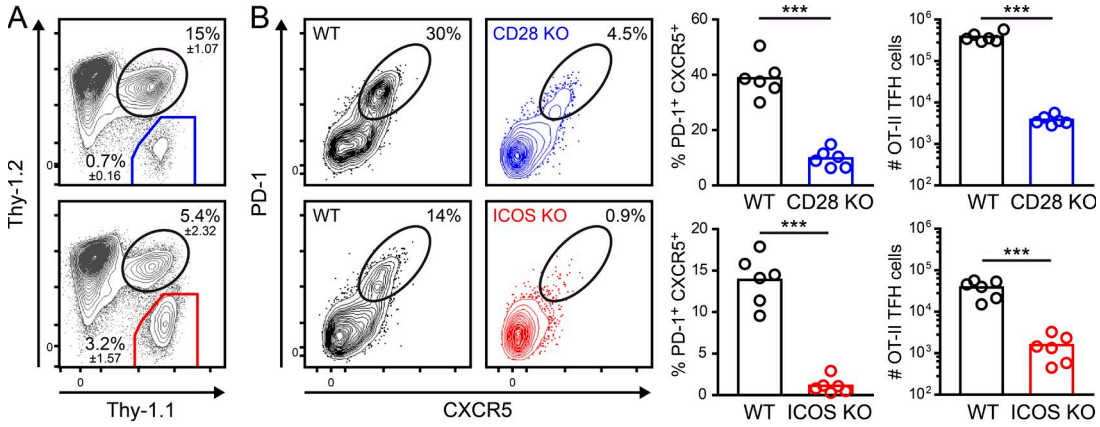

Figure 1. CD28 and ICOS are both important for the generation of a TFH cell population on day 8. WT (Thy-1.1+ 1.2+, black) and CD28 KO (Thy-1.1+, blue) or WT and ICOS KO (Thy-1.1+, red) OT-II T cells were co-transferred together with B1-8i B cells into C57BL/6 recipients (Thy-1.2+). Recipients were subcutaneously immunized with NP-OVA on the following day and draining lymph nodes were analyzed on day 8 after immunization by flow cytometry. (A) Representative contour plots (gated on CD4+ T cells) showing the expansion of WT and KO T cells (indicated as percentage ± SD of all CD4+ T cells). (B) Gated OT-II T cells were analyzed for a TFH phenotype defined by expression of CXCR5 and PD-1. Representative contour plots and graphs showing frequency and absolute numbers of TFH cells with dots representing individual mice and bars indicating the mean. Data are representative of four independent experiments with six animals per group. ***, $P < 0.001$.

used a blocking antibody against ICOS-L to interrupt ICOS signaling in already differentiated TFH cells. For comparison, the CD28 pathway was blocked using a CTLA-4–Ig fusion protein that binds to the receptors B7-1 (CD80) and B7-2 (CD86) with high affinity (Linsley et al., 1992). Both reagents effectively blocked co-stimulatory signals via ICOS or CD28, as application at early times (day −1 to +1 after immunization) led to similar results in early T cell responses (day 3) as obtained with corresponding KO mice (unpublished data). Blockade of the CD28 pathway starting from day 6 did not have any effects on the frequency of CXCR5+ PD-1+ cells 48 h later. In contrast, blockade of ICOS signaling resulted in an almost complete loss of the TFH phenotype (Fig. 3 A).

The loss of TFH cells could be explained by selective death of TFH cells, a reversion of their phenotype toward non-TFH effector cells, or T cell egress from the draining lymph node. As blocking of ICOS signaling did not increase the percentage of apoptotic cells (Fig. 3 B), we devised a system to explicitly track the fate of TFH cells. We sorted antigen-specific TFH cells (CXCR5+ PD-1+) from a day 7 immune response to high purity (> 96%) and transferred them into secondary hosts. ICOS signaling was blocked and the phenotype of the transferred cells was analyzed 48 h later (Fig. 3 C). As before, most of the TFH cells had lost their phenotype, but the absolute number of transgenic T cells in the TFH retransfer group had not changed upon blockade. Hence, these experiments showed that TFH cells do not die or emigrate from the draining lymph node, but revert their phenotype if they do not receive continuous signals via ICOS.

Late ICOS-L blockade results in collapse of an established GC response

Which functional consequences does this loss of phenotype have for an ongoing immune response? To analyze the fate of antigen-specific GC B cells, we co-transferred NP-specific B cells from B1-8i mice together with OT-II T cells. ICOS-L blockade on day 6 reduced the frequency of antigen-specific peanut agglutinin (PNA)+ GL7+ GC B cells (Fig. 4 A) as well as serum levels of antigen-specific IgG1 and IgG2a (Fig. 4 B) by more than 75 and 50%, respectively. Histological analysis revealed that the majority of the OT-II T cells in the B cell follicle had relocated to the T cell zone (Fig. 4 C), whereas blocking of the CD28 pathway did not have an effect on the B cell response (Fig. 4 B) or on T cell localization (Fig. 4 C).

These experiments demonstrate a reversal of the functions of CD28 and ICOS between early and late phases of an immune response. Whereas CD28 is important for early TFH differentiation, continuous ICOS signaling is required for maintenance of the TFH phenotype. If ICOS co-stimulation is interrupted, TFH cells lose their phenotype and migrate back to the T cell zone, which results in a collapse of the GC reaction.

ICOS regulates TFH homing molecules

To gain a deeper understanding of this phenotype reversion, TFH cells were analyzed 20 h after blocking ICOS-L, while conversion was still in progress. After this short period, the intensity of CXCR5 and PD-1 staining was already diminished on TFH cells (Fig. 5 A). At the same time, the expression of the T cell zone homing receptors CCR7 and P-selectin glycoprotein ligand-1 (PSGL-1; Haynes et al., 2007; Veerman et al., 2007; Poholek et al., 2010) increased (Fig. 5 B). Importantly, expression of the transcription factors Bcl-6 and *c-Maf* by TFH cells was unchanged. *Ascl2* was slightly reduced by only 16%, which is unlikely to have any biological significance (Fig. 5, B and C). This demonstrates that ICOS primarily regulates the expression of TFH homing markers and not TFH-related transcription factors. However, expression of *Tbx21*

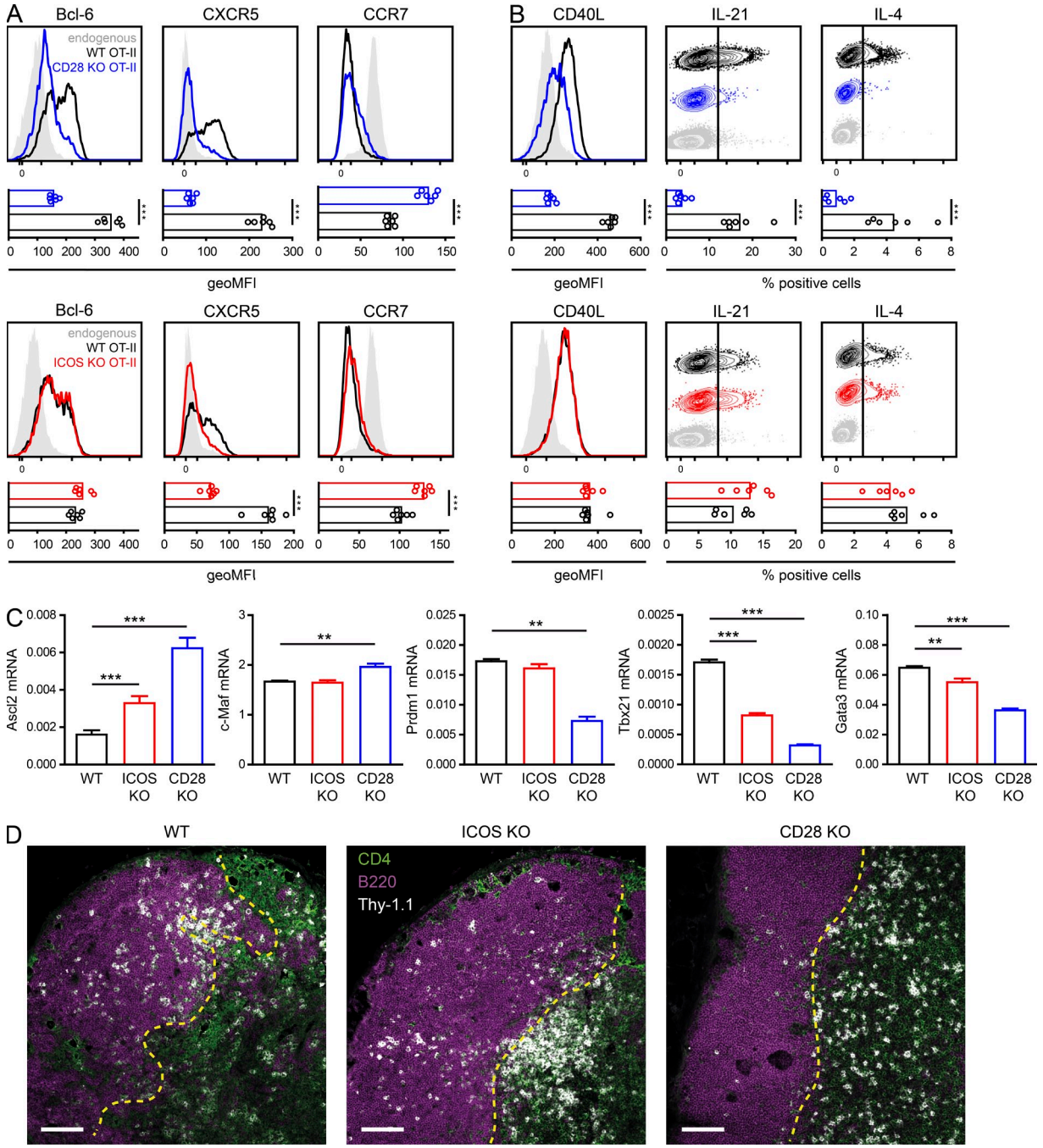

Figure 2. CD28 but not ICOS regulates early key events of TFH cell differentiation. WT (black) and CD28 KO (blue) or ICOS KO (red) OT-II cells were either co-transferred (A and B) or transferred separately (C and D) into C57BL/6 recipients subcutaneously immunized with NP-OVA. Draining lymph nodes were analyzed on day 3 after immunization. (A) Expression of Bcl-6, CXCR5, and CCR7 analyzed by flow cytometry and displayed as representative histograms and as bar graph with the geometric mean fluorescence intensity (geoMFI). Endogenous $CD4^+$ T cells are shown in gray. Dots represent individual mice and bars indicate the mean. (B) Expression of CD40L was evaluated ex vivo by intracellular staining without restimulation and IL-21 and IL-4 were assessed after short-term restimulation with OVA peptide. Representative flow cytometry data and geoMFI or percentage of positive cells are shown. (C) WT or KO OT-II T cells were sorted from draining lymph nodes (pool from 20 animals) by magnetic and flow sorting for Thy-1.1^+ cells for the preparation of RNA. Expression of *Ascl2*, *c-Maf*, *Prdm1*, *Tbx21*, and *Gata3* mRNA was measured by quantitative RT-PCR (expression relative to *Hprt*; mean ± SEM from triplicates and two independent experiments). (D) Representative histological pictures of draining lymph nodes showing the T cell zone ($CD4^+$, green), B cell follicle ($B220^+$, magenta), and antigen-specific T cells (Thy-1.1^+, white). The yellow dashed line demarcates the border between the T cell zone and the B cell follicle. Bars, 100 µm. Representative data from two (mRNA, cytokines, and histology) or four (all other) experiments. **, $P < 0.01$; ***, $P < 0.001$.

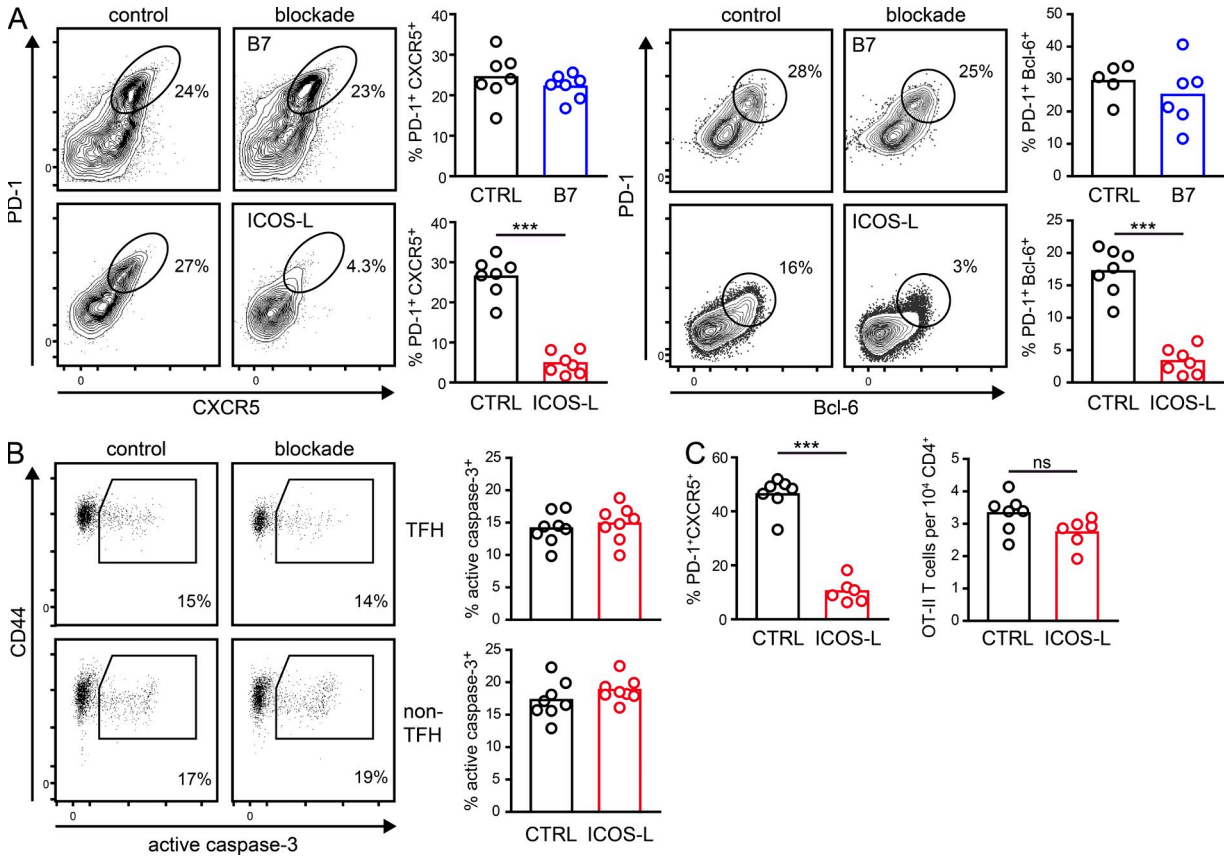

Figure 3. ICOS but not CD28 is important for maintenance of TFH cells. (A and B) Thy-1.1+ OT-II T cells were transferred into C57BL/6 recipients that were immunized subcutaneously with NP-OVA on the following day. Starting from day 6 (A) or day 7 (B) after immunization, CD28 or ICOS signaling was blocked using CTLA-4–Ig or anti–ICOS-L antibody, respectively. OT-II T cells from draining lymph nodes were analyzed by flow cytometry on day 8 after immunization. (A) Expression of CXCR5/PD-1 or Bcl-6/PD-1 on OT-II T cells is shown as representative contour plots and bar graphs indicating the percentage of cells with a TFH phenotype. (B) Apoptosis of OT-II TFH (CXCR5+ PD-1+) or non-TFH (CXCR5− PD-1−) CD4+ T cells was analyzed by staining for active caspase-3. Results are shown as representative dot plots and bar graphs. (C) Antigen-specific TFH cells were sorted on day 7 according to CXCR5 and PD-1 expression and transferred into secondary hosts which had been immunized 7 d before. ICOS-L was blocked for 48 h before analysis of draining lymph nodes by flow cytometry. Frequency of TFH cells and total OT-II T cells was assessed. Results are representative for eight (ICOS-L blockade), three (B7 blockade), or two (apoptosis, TFH retransfer) independent experiments with six to eight animals per group. Dots represent individual mice and bars indicate the mean. ***, $P < 0.001$.

and *Gata3* significantly increased upon blocking ICOS-L, indicating the conversion of TFH cells into other Th subsets.

ICOS down-regulates the zinc-finger transcription factor Klf2

To investigate which transcription factors are regulated by ICOS-mediated signaling and might play a role for the maintenance of the TFH phenotype, we performed a transcriptome analysis. Antigen-specific TFH cells were sorted from draining lymph nodes after 6 h of blocking ICOS-L. Comparing the ICOS-L blockade with the control group, we observed no difference for any of the transcription factors known to be important for TFH cell differentiation including Bcl-6, Blimp-1, Irf4, Ascl2, and c-Maf. However, the zinc-finger transcription factor Klf2 showed up as one of the most significantly differentially regulated genes. This transcription factor is highly expressed in naive T cells, strongly down-regulated shortly after T cell receptor triggering, and maintained on a lower level in activated T cells (Fig. 6 A). The sixfold lower expression of *Klf2* in TFH versus non-TFH cells made it a particularly interesting target for further analyses (Fig. 6 B). Upon blocking ICOS-L, *Klf2* was rapidly up-regulated by a factor of 3.5, approaching the expression levels of non-TFH cells (Fig. 6 C). Klf2 was originally described as a factor controlling thymocyte egress via up-regulation of sphingosine-1-phosphate receptor 1 (S1PR1) and CD62L (Carlson et al., 2006). Therefore, we analyzed these target genes on antigen-specific TFH cells after ICOS-L blockade. CD62L and S1PR1 were up-regulated 1.6- and 2.8-fold, respectively, whereas CD69, which is inversely regulated to S1PR1 (Shiow et al., 2006), was reduced by 30% (Fig. 6 D). In contrast, blockade of the CD28 pathway did

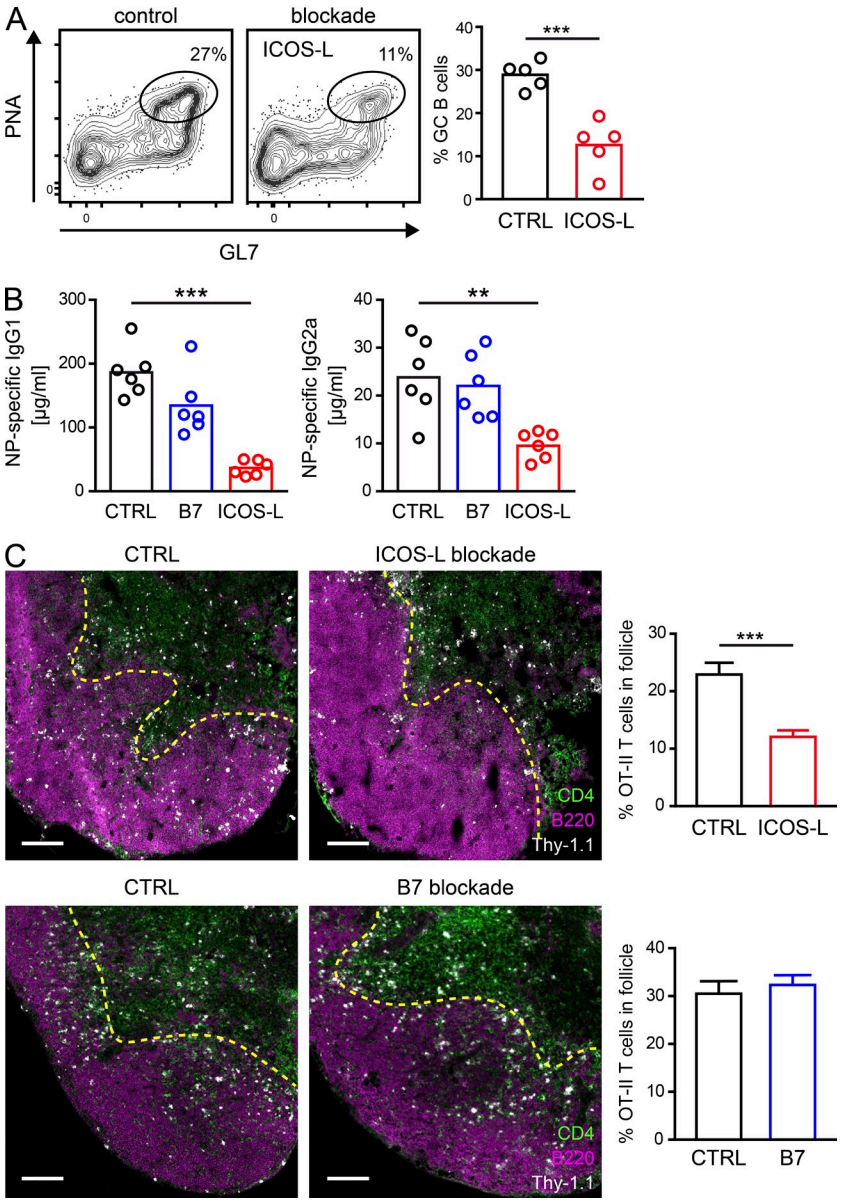

Figure 4. Late ICOS-L blockade results in collapse of an established GC response. OT-II T cells and B1-8i B cells were co-transferred into C57BL/6 recipients immunized subcutaneously with NP-OVA. ICOS-L or B7 blockade was started on day 6 after immunization. (A) Draining lymph nodes were analyzed by flow cytometry on day 10 for antigen-specific GC B cells (CD45.1$^+$ PNA$^+$ GL7$^+$). Representative flow cytometry plots and bar graphs indicating the frequency of GC B cells are shown. (B) Serum levels of NP-specific IgG1 and IgG2a were analyzed on day 13 by ELISA. (C) Histological analysis of draining lymph nodes on day 10. The T cell zone (CD4$^+$) is shown in green, B cell zone (B220$^+$) in magenta, and OT-II T cells (Thy-1.1$^+$) in white. The yellow dashed lines demarcate the border between the T cell zone and the B cell follicle. Bars, 200 µm. Bar graphs show the frequency of transgenic T cells in the B cell area by analyzing whole lymph node sections from 6 different depths of the lymph node. Representative result from three (A) or two (B) independent experiments with five to six animals per group and (C) pooled data from two independent experiments with four animals per group. Dots represent individual mice, bars indicate the mean and error bars the SEM. ***, $P < 0.001$.

not change Klf2 expression or expression of any of the latter receptors (Fig. 6 E).

To find out how both co-stimulators regulate Klf2 expression during early T cell activation, we analyzed Klf2 expression in antigen-specific ICOS and CD28 KO T cells on day 3 (same setup as in Figs. 1 and 2). Interestingly, the roles of ICOS and CD28 were reversed at these early time points (Fig. 6 F). Whereas *Klf2* expression was 9-fold higher in CD28 KO T cells, lack of ICOS co-stimulation increased *Klf2* by a factor of 2.3 only. However, lack of both co-stimulatory pathways (transfer of ICOS KO T cells into B7 KO recipients) resulted in a strong synergistic effect (21-fold higher expression), indicating that ICOS signals can be partially replaced by CD28 during early T cell activation.

To investigate whether ICOS and Klf2 are also crucial for maintenance of human TFH cells, we analyzed T cells from tonsillar tissue. Interestingly, all the aforementioned molecules regulated by ICOS correlated with the degree of ICOS expression on tonsillar T cells (Fig. 7 A), indicating a regulation by ICOS co-stimulation. To prove the functional relevance, we blocked ICOS-signaling in an in vitro T/B cell cooperation assay. As in the mouse model, *Klf2* mRNA increased more than 4.5-fold after only 6 h of ICOS-L blockade (Fig. 7 B). Similarly, *S1pr1* and *Sell* (encoding CD62L) levels increased 2.8- and 2.3-fold, respectively, whereas *Cxcr5* expression significantly decreased. Expression of *Bcl-6* was even slightly enhanced, whereas *Ascl2* expression was minimally reduced, both in a range which should have no biological effects (Fig. 7 B).

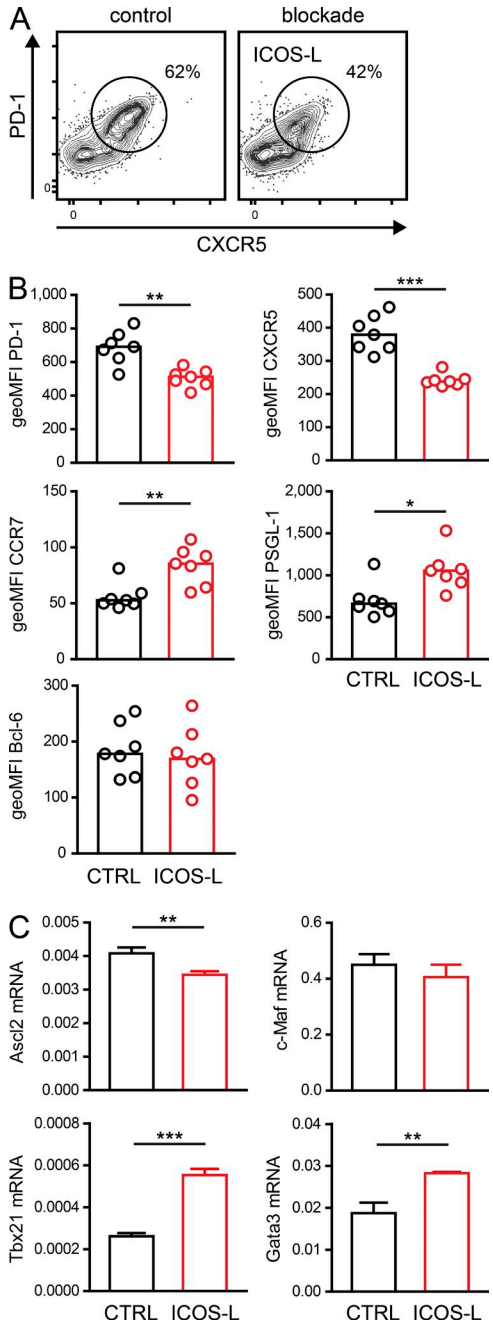

Figure 5. Interruption of ICOS signaling results in rapid reversion of the TFH phenotype. OT-II T cells were transferred into C57BL/6 recipients, which were immunized subcutaneously with NP-OVA on the following day. On day 7 after immunization, recipients were treated with anti–ICOS-L or control antibody (CTRL). (A) Antigen-specific Thy-1.1$^+$ CXCR5$^+$ PD-1$^+$ cells were analyzed by flow cytometry after 20 h of blockade. (B) Expression of CCR7, PSGL-1, and Bcl-6 on gated TFH cells is shown as geoMFI; each dot represents an individual animal and bars indicate the mean. Representative experiment out of three, with seven animals per group. (C) Antigen-specific TFH cells (Thy-1.1$^+$ CXCR5$^+$ PD-1$^+$; draining lymph nodes pooled from 20 animals) were sorted 6 h after blockade for preparation of RNA. Expression of *c-Maf*, *Ascl2*, *Gata3*, and *Tbx21* was measured by quantitative RT-PCR. Shown is the mean (± SEM) expression relative to β2-microglobulin from two independent experiments with three technical replicates each. *, P < 0.05; **, P < 0.01; ***, P < 0.001.

Overexpression of Klf2 in T cells results in loss of TFH cells and terminates the GC response

To test whether suppression of Klf2 is the major mechanism by which ICOS regulates TFH cell differentiation, we overexpressed Klf2 in antigen-specific T cells. OT-II T cells were retrovirally transduced with a vector coding for Klf2 and GFP or a control vector with GFP only. 1 d after infection, overexpression of Klf 2 in vitro resulted in a 1.7- and 2.5-fold increased expression of its known target genes CD62L and *S1pr1*, respectively (Fig. 8 A). At the same time, expression levels of CD44 and other activation markers, like OX-40 and 4-1BB, were unaltered or even increased, which shows that overexpression of Klf2 did not result in a general block of T cell activation. Importantly, *Bcl-6*, *c-Maf*, *Prdm1*, and *Ascl2* were expressed equally in both groups, demonstrating that overexpression of Klf2 did not directly regulate key factors of TFH cell differentiation. To substantiate these results, we stimulated T cells from inducible Klf2 KO mice. As expected, *Klf2* mRNA and the known downstream target *S1pr1* were strongly reduced, whereas expression of the TFH-related transcription factors *Bcl-6*, *c-Maf*, and *Ascl-2* remained unchanged (Fig. 8 B).

Normally, it is not possible to induce CXCR5 on stimulated T cells in vitro. The only way to do so is by overexpression of Ascl2 (Liu et al., 2014). To analyze the interplay of Ascl2 and Klf2 in the regulation of CXCR5, we performed double-transfection experiments with retroviral vectors encoding both transcription factors. Overexpression of Ascl2 alone resulted in a more than fivefold up-regulation of CXCR5 (Fig. 8 C). Interestingly, Klf2 was able to block this Ascl-2–induced expression almost completely. This demonstrates that Klf2 does not regulate early factors of TFH cell differentiation like Bcl-6 and Ascl2, but counteracts the downstream events of these early factors.

To test for TFH cell differentiation in vivo, retrovirally transduced OT-II cells were transferred into recipient mice, which were injected subcutaneously with cognate antigen. Analysis of antigen-specific T cells 42 h later revealed lower expression of CXCR5 and PD-1, as well as increased expression of PSGL-1 and CD62L. On day 6 after transfer, the frequency of CXCR5$^+$ PD-1$^+$ TFH cells was reduced fourfold among cells overexpressing Klf2, whereas expression of PSGL-1 and CD62L was increased (Fig. 8, D and E).

To investigate whether Klf2 overexpression in fully matured TFH cells is able to reverse the TFH phenotype, we developed a tamoxifen-inducible expression system. 48 h after induction of Klf2 overexpression, half of the TFH cells had lost their phenotype according to CXCR5/PD-1, PSGL-1, and CD62L expression (Fig. 9 A). In addition, the number of antigen-specific GC B cells was reduced more than twofold two days later (Fig. 9 B).

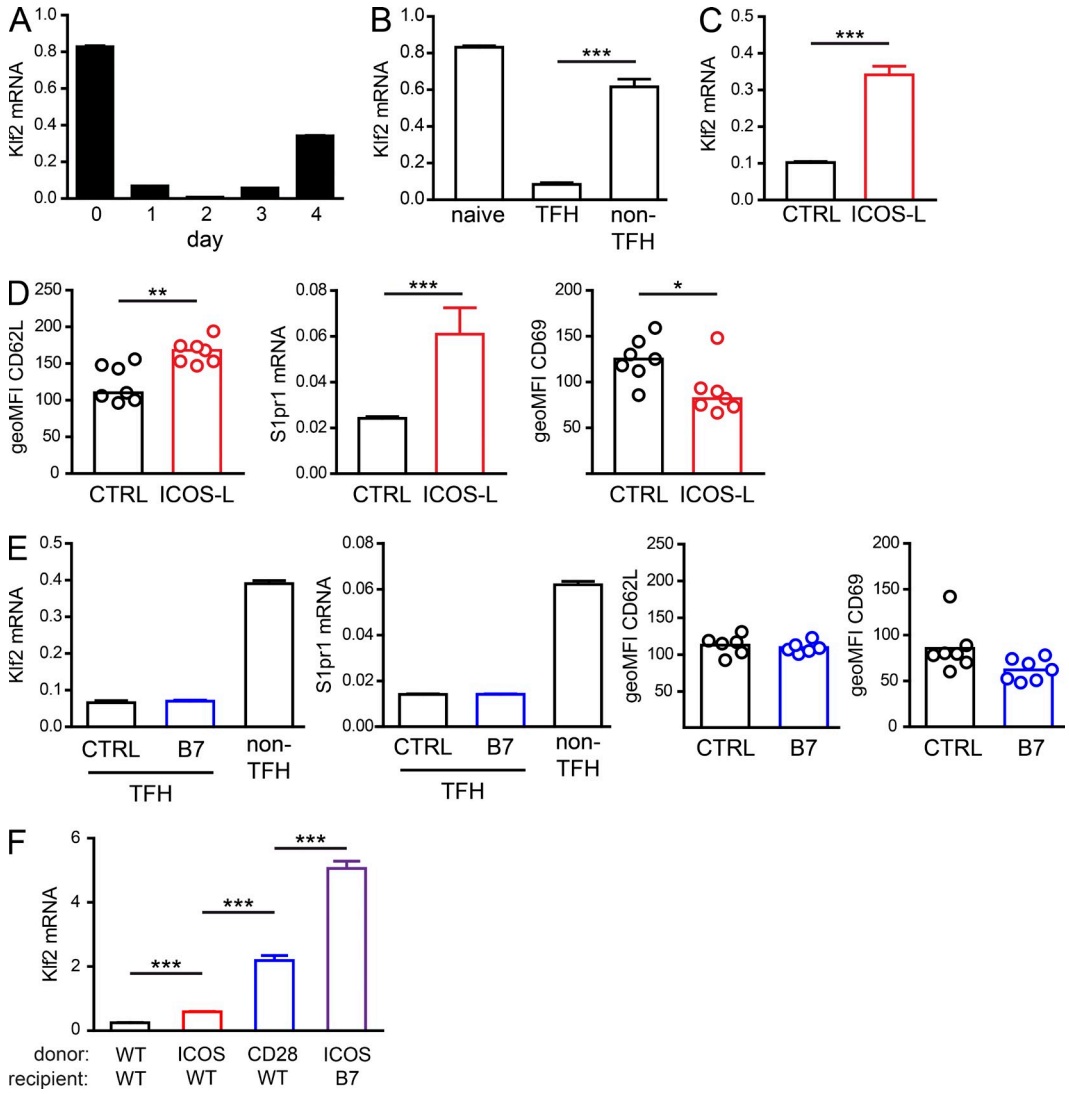

Figure 6. ICOS down-regulates Klf2 to maintain TFH cell homing markers. (A) OT-II splenocytes were stimulated in vitro with $OVA_{323-339}$ peptide. T cells were sorted from cultures at the indicated times and Klf2 mRNA was quantified by RT-PCR. (B) Recipients of Thy-1.1+ OT-II T cells were immunized with cognate antigen and antigen-specific Thy-1.1+ CXCR5/PD-1 double-positive (TFH) or double-negative cells (non-TFH) were sorted from draining lymph nodes on day 8. Klf2 expression was analyzed by quantitative RT-PCR. For comparison, Klf2 expression in naive OT-II T cells is shown. (C–E) Thy-1.1+ OT-II T cells were transferred into C57BL/6 recipients immunized subcutaneously with NP-OVA. On day 7 after immunization, recipients were treated with anti–ICOS-L, CTLA-4–Ig, or control reagents (CTRL). Antigen-specific TFH cells (Thy-1.1+ CXCR5+ PD-1+) from draining lymph nodes were sorted for preparation of RNA 6 h after blockade and analyzed by flow cytometry 20 h after blockade, respectively. (C) *Klf2* expression analyzed by quantitative RT-PCR after ICOS-L blockade. (D) CD62L and CD69 expression analyzed by flow cytometry (MFI) and *S1pr1* expression analyzed by quantitative RT-PCR after ICOS-L blockade. (E) Expression of *Klf2* and *S1pr1* by RT-PCR and CD62L and CD69 by flow cytometry after CTLA-4–Ig blockade. All quantitative RT-PCR data are mean values (± SEM) from three experiments with three technical replicates each and β2-microglobulin as housekeeping gene. Flow cytometry data are a representative result from three (ICOS-L blockade) or two (B7 blockade) independent experiments with seven animals per group. (F) WT, ICOS KO, or CD28 KO OT-II T cells were transferred into C57BL/6 recipients or ICOS KO OT-II T cells were transferred into CD80/86 (B7) KO recipients. Transgenic T cells were sorted from pools of draining lymph nodes 3 d after immunization with NP-OVA. *Klf2* mRNA was quantified by RT-PCR (expression relative to Hprt; mean ± SEM from triplicates and two independent experiments). Dots represent individual mice, bars indicate the mean, and error bars represent the SEM. *, $P < 0.05$; **, $P < 0.01$; ***, $P < 0.001$.

To address the reverse situation to Klf2 overexpression, we adoptively transferred antigen-specific T cells from tamoxifen-inducible Klf2 KO mice. Induction of Klf2 knockout during early T cell activation (day 2) resulted in a strong reduction of antigen-specific T cells in the draining lymph nodes (unpublished data) as reported previously (Sebzda et al., 2008). Therefore, we decided to induce Klf2 knockdown on day 4. In addition, we blocked ICOS-L starting on day 6, to test whether the TFH cell phenotype can still be reverted when the major ICOS downstream target is not expressed. As

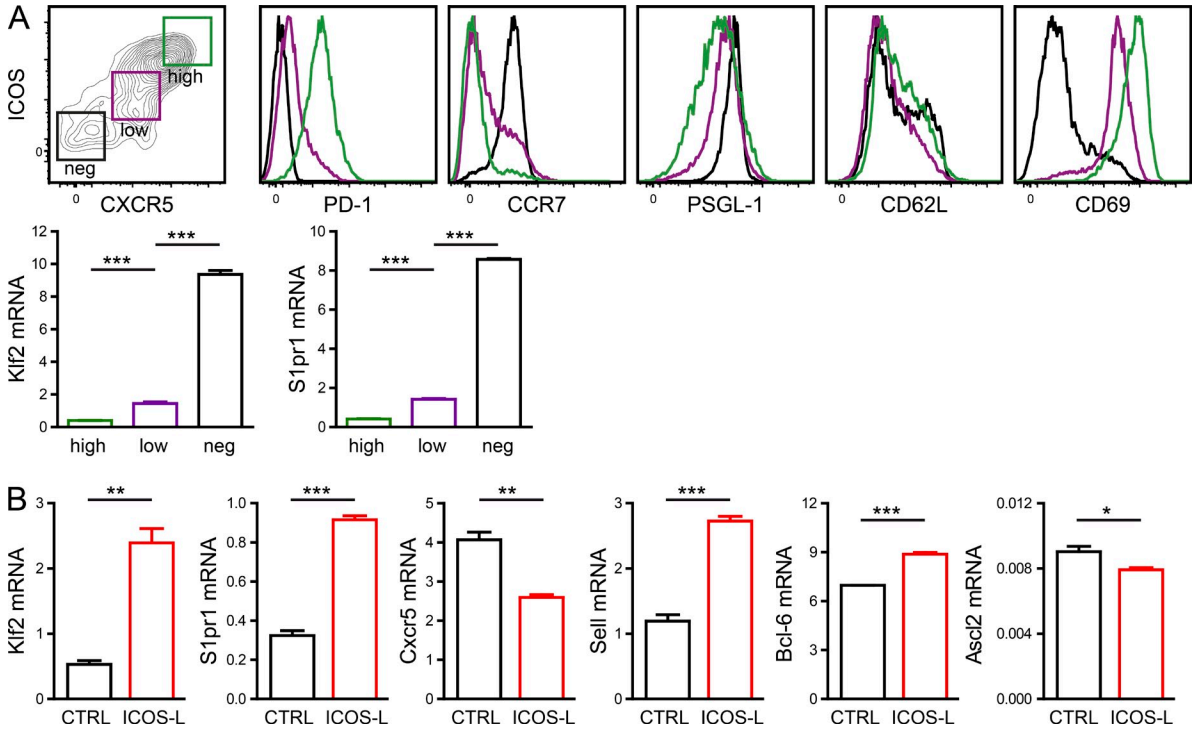

Figure 7. Analysis of human tonsillar TFH cells for ICOS-regulated genes. (A) CD3$^+$ CD4$^+$ T cell populations from human tonsils were defined based on differential expression of CXCR5 and ICOS (negative, low, and high). Expression of PD-1, CCR7, PSGL-1, CD62L, and CD69 on these different populations was analyzed by flow cytometry. Expression of *Klf2* and *S1pr1* was assessed in sorted populations by quantitative RT-PCR (bar graphs showing expression relative to *Hprt*; mean ± SEM from triplicates). (B) Tonsillar mononuclear cells were cultured in the presence of staphylococcal enterotoxin B (SEB) and blocking antibody against ICOS-L or isotype control. After 6 h, CXCR5$^+$ ICOS$^+$ CD4$^+$ T cells were sorted and expression of *Klf2*, *S1pr1*, *Cxcr5*, *Sell* (endcoding CD62L), *Bcl-6*, and Ascl2 mRNA was analyzed by quantitative RT-PCR (expression relative to *Hprt*; mean ± SEM from triplicates). One representative experiment out of two is shown. *, $P < 0.05$, **, $P < 0.01$; ***, $P < 0.001$.

expected, CD62L and PSGL-1 were expressed on a lower level in the Klf2 knockdown situation. Most importantly, expression of TFH cell homing receptors was no longer changed by ICOS-L blockade (Fig. 9 C). Unexpectedly, knockdown of Klf2 did not result in enhanced but in diminished numbers of CXCR5$^+$ PD-1$^+$ TFH cells (Fig. 9 C). This indicates that TFH cells require low, but not absent, levels of Klf2 to maintain their phenotype.

We identified Klf2 as the major ICOS-regulated transcription factor that determines the fate of TFH cells because overexpression of Klf2 resulted in a similar phenotype as blocking of the ICOS signaling pathway and expression of TFH-related molecules was no longer changed by ICOS-L blockade in Klf2 KO mice.

ICOS is more potent to regulate Klf2 via Foxo1 than CD28

To obtain a more comprehensive mechanistic insight into how ICOS co-stimulation regulates Klf2 and TFH homing molecules, we performed an in-depth analysis of the involved signaling pathways. An in vitro co-stimulation system with purified T cells and plate-bound antibodies against CD3 and ICOS or CD28 revealed that ICOS co-stimulation reduced *Klf2* mRNA levels eightfold compared with stimulation with anti-CD3 alone (Fig. 10 A). In comparison, CD28 co-stimulation had only minor effects on Klf2 expression.

It has recently been shown that Klf2 is a direct downstream transcriptional target of Foxo1 (Fabre et al., 2008; Kerdiles et al., 2009). Because CD28 regulates Foxo1 via the phosphatidylinositol-3-kinase (PI3K) pathway (Hedrick et al., 2012), and the same has recently been shown for ICOS (Xiao et al., 2014), we compared how both co-stimulatory pathways activate Foxo1. Using the in vitro co-stimulation system, we could show that ICOS substantially enhanced phosphorylation and subsequent translocation of nuclear Foxo1 to the cytosol, whereas CD28 co-stimulation had only minor effects (Fig. 10, B and C).

Klf2 directly binds to *Cxcr5*, *Selplg*, and *Ccr7*

To analyze binding of Klf2 to regulatory elements of the genes influenced by ICOS blocking, namely *Ccr7*, *S1pr1*, *Selplg* (encoding PSGL-1), and *Cxcr5* (Fig. 10 D), we performed chromatin immunoprecipitation (ChIP). It has already been shown that Klf2 directly regulates CD62L and S1pr1 (Carlson et al., 2006; Bai et al., 2007), and we used the latter as a positive control. Precipitation of DNA bound to Klf2 resulted in a more than fivefold enrichment of sequences from the *S1pr1*,

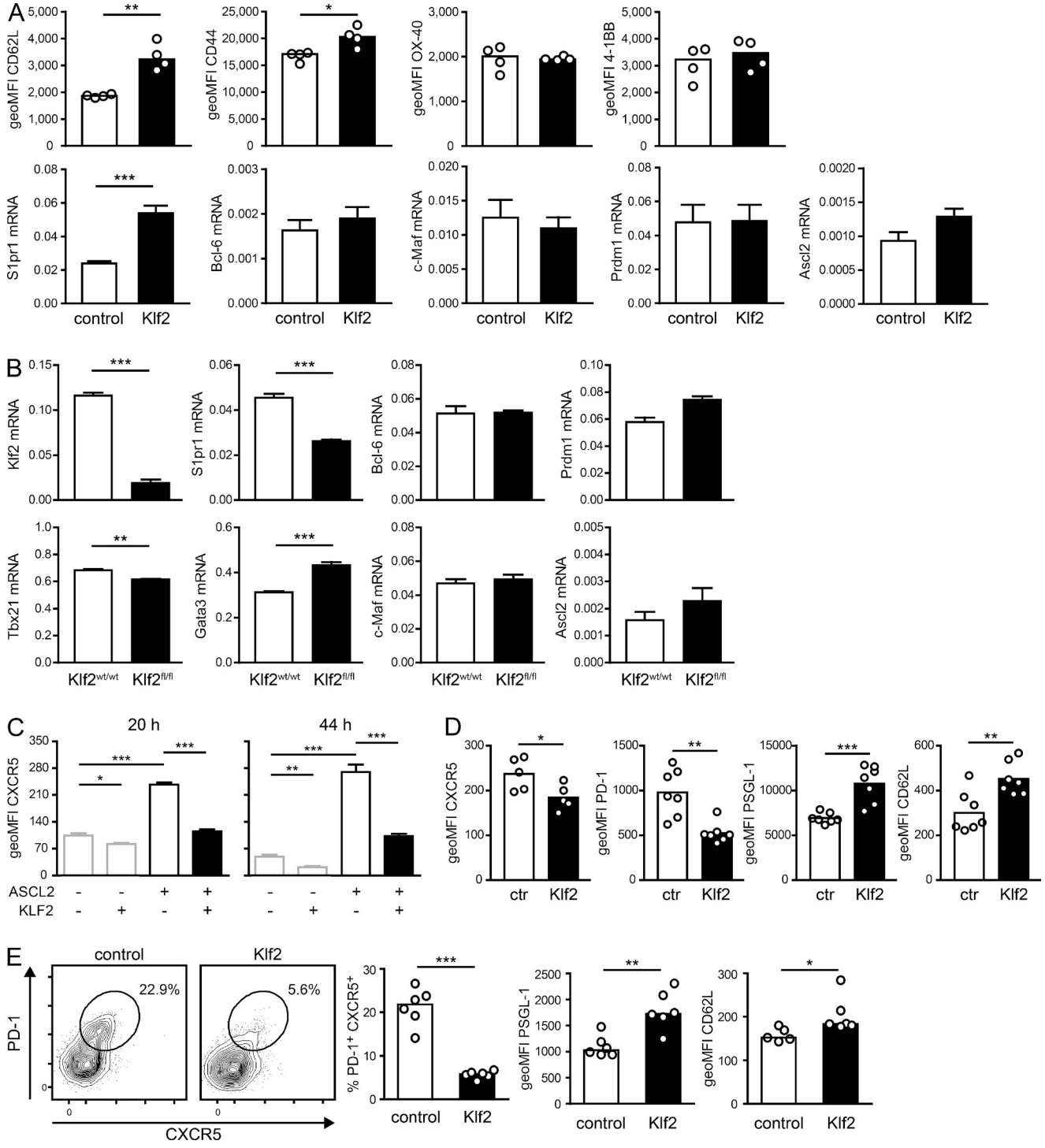

Figure 8. Overexpression identifies Klf2 as a novel repressor of TFH cell differentiation. (A) OT-II T cells were retrovirally transduced with Klf2 cDNA or an empty control vector encoding GFP only. 24 h after infection, the expression of CD62L, CD44, OX-40, and 4-1BB on Thy-1.1$^+$ GFP$^+$ cells was analyzed by flow cytometry in vitro (representative results from two independent experiments with quadruplicate wells). In addition, GFP$^+$ cells were sorted and expression of *S1pr1*, *Bcl-6*, *c-Maf*, *Prdm1*, and *Ascl2* was measured by quantitative RT-PCR (relative to β2-microglobulin; mean ± SEM of two independent experiments with three technical replicates each). (B) OT-II x CreER^{T2} x Klf2$^{wt/wt}$ or Klf2$^{fl/fl}$ splenocytes were stimulated with OVA peptide in the presence of tamoxifen (TMX). T cells were sorted after 24 h and analyzed by quantitative RT-PCR (relative to *Hprt*; mean ± SEM of two independent experiments with three technical replicates each) for expression of *Klf2*, *S1pr1*, *Bcl-6*, *Prdm1*, T*bx21*, *Gata3*, c-*Maf*, and *Ascl2*. (C) OT-II T cells were retrovirally transfected with plasmids encoding Ascl2 (hu CD4 as reporter) and Klf2 (GFP reporter) or empty vector controls. After 20 and 44 h, expression of CXCR5 was analyzed by flow cytometry. Representative experiment out of two with quadruplicates. (D and E) OT-II T cells were retrovirally transduced

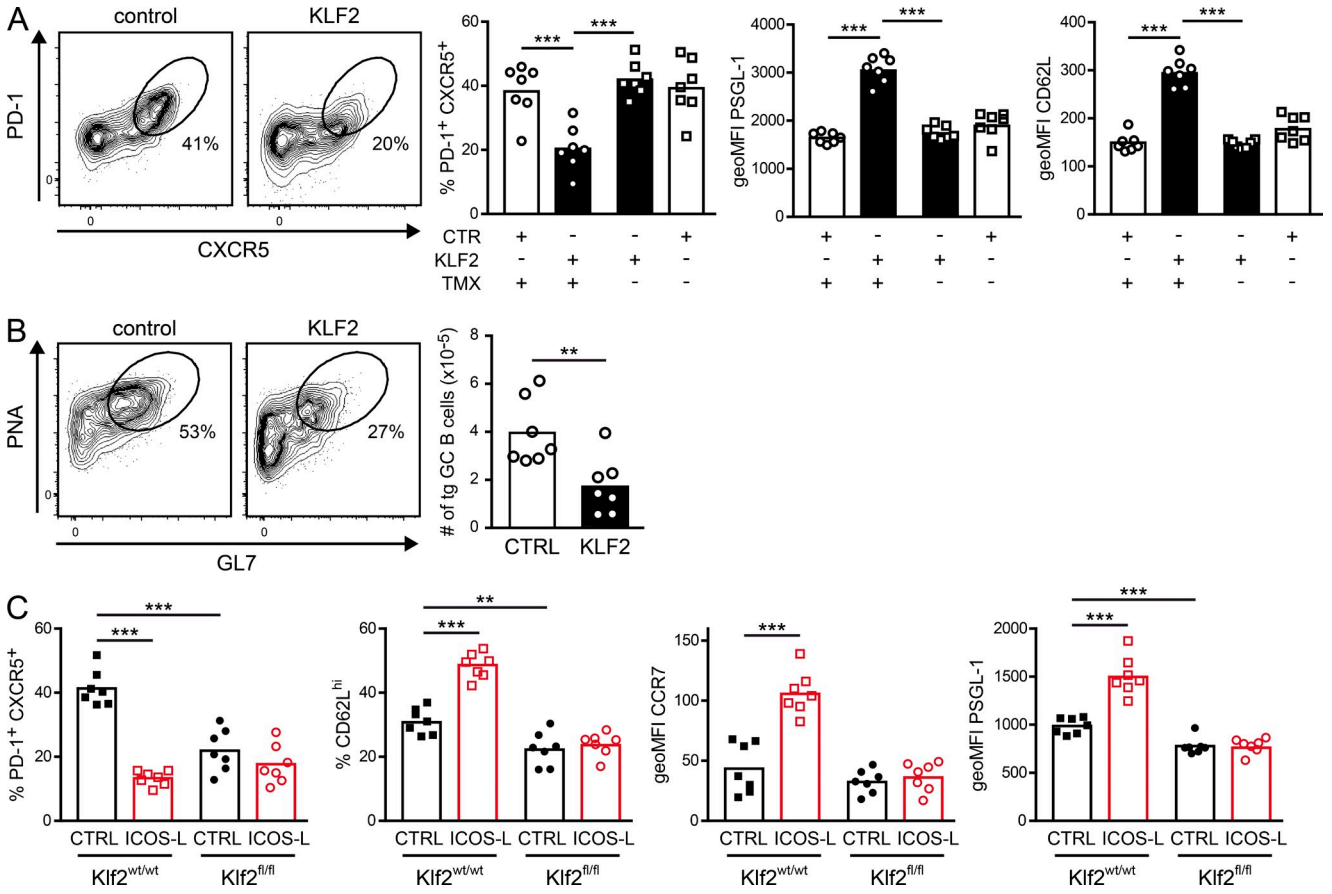

Figure 9. Induced overexpression of Klf2 results in loss of TFH cells and termination of the GC response. (A and B) Thy-1.1+ OT-II x CreER^{T2} T cells were transduced with either an empty (control) retroviral vector or a vector containing a loxP-flanked dsRed stop cassette in front of the *Klf2* coding region, preventing expression until the cassette is removed by (tamoxifen-induced) Cre-mediated excision. After a 20-h in vitro culture, dsRed-expressing cells were sorted and transferred together with NP-specific CD45.1+ B1-8i B cells into B6 WT (A) or B6 CD28 KO (B) recipients (to exclude effects from endogenous TFH cells). Recipients were immunized with NP-OVA on the same day. Four days later, Klf2 overexpression was induced by tamoxifen (TMX)-mediated excision of the dsRed cassette. (A) Flow cytometric analysis of OT-II T cells (Thy-1.1+) for expression of CXCR5, PD-1, PSGL-1, and CD62L on day 6. Shown are representative plots for PD-1/CXCR5 expression and bar graphs indicating percentage of PD-1+ CXCR5+ OT-II cells and geoMFI expression of PSGL-1 and CD62L. (B) Analysis of antigen-specific (CD45.1+) B cells on day 8. Representative plots for transgenic (CD45.1+) B cells with a GC phenotype (PNA+ GL7+) and bar graphs indicating the absolute number of GC B cells are shown. (C) OT-II x CreER^{T2} x Klf2$^{fl/fl}$ T cells were transferred into B6 mice subsequently immunized with NP-OVA. On day 4 after immunization, Klf2 knockdown was induced by tamoxifen. On day 6 and 7, ICOS-L was blocked using a monoclonal antibody. OT-II T cells from draining lymph nodes were analyzed on day 8 for expression of PD-1/CXCR5, CD62L, CCR7, and PSGL-1. Dots represent individual mice and bars indicate the mean. Representative experiments out of two, with five to seven animals per group. *, $P < 0.05$; **, $P < 0.01$; ***, $P < 0.001$.

Cxcr5, *Selplg*, and *Ccr7* promoters (Fig. 10 E). A second potential Klf2 binding site in the intergenic region of the *Cxcr5* gene (Cxcr5 up) was not addressed by Klf2. To functionally test the identified Klf2-binding site in the *Cxcr5* promoter, we performed a luciferase expression assay. Overexpression of Klf2 resulted in a fourfold reduction of luciferase activity, demonstrating that Klf2 negatively regulates CXCR5 (Fig. 10 F).

Collectively, we could unravel the complete signaling cascade upstream and downstream of Klf2. ICOS represses Klf2 via Foxo1 and Klf2 acts as a repressor of *Cxcr5* and activator of *S1pr1*, *Ccr7*, and *Selplg*.

DISCUSSION

CD28 and ICOS are two structurally and functionally closely related T cell co-stimulators (Hutloff et al., 1999). In this study, we analyzed the contribution of both molecules to specific phases of TFH cell differentiation and found a clear-cut functional division. Although CD28 controls early events

with Klf2 cDNA or control vector and transferred into C57BL/6 recipient mice immunized on the same day with NP-OVA. After 42 h (D) or 6 d (E), antigen-specific GFP+ CD4+ T cells were analyzed for the TFH phenotype by flow cytometry. Representative contour plots for CXCR5/PD-1 expression on day 6 and bar graphs with expression of PD-1, CXCR5, PSGL-1, and CD62L are shown. Representative experiment out of three with six to seven animals per group. *, $P < 0.05$; **, $P < 0.01$; ***, $P < 0.001$.

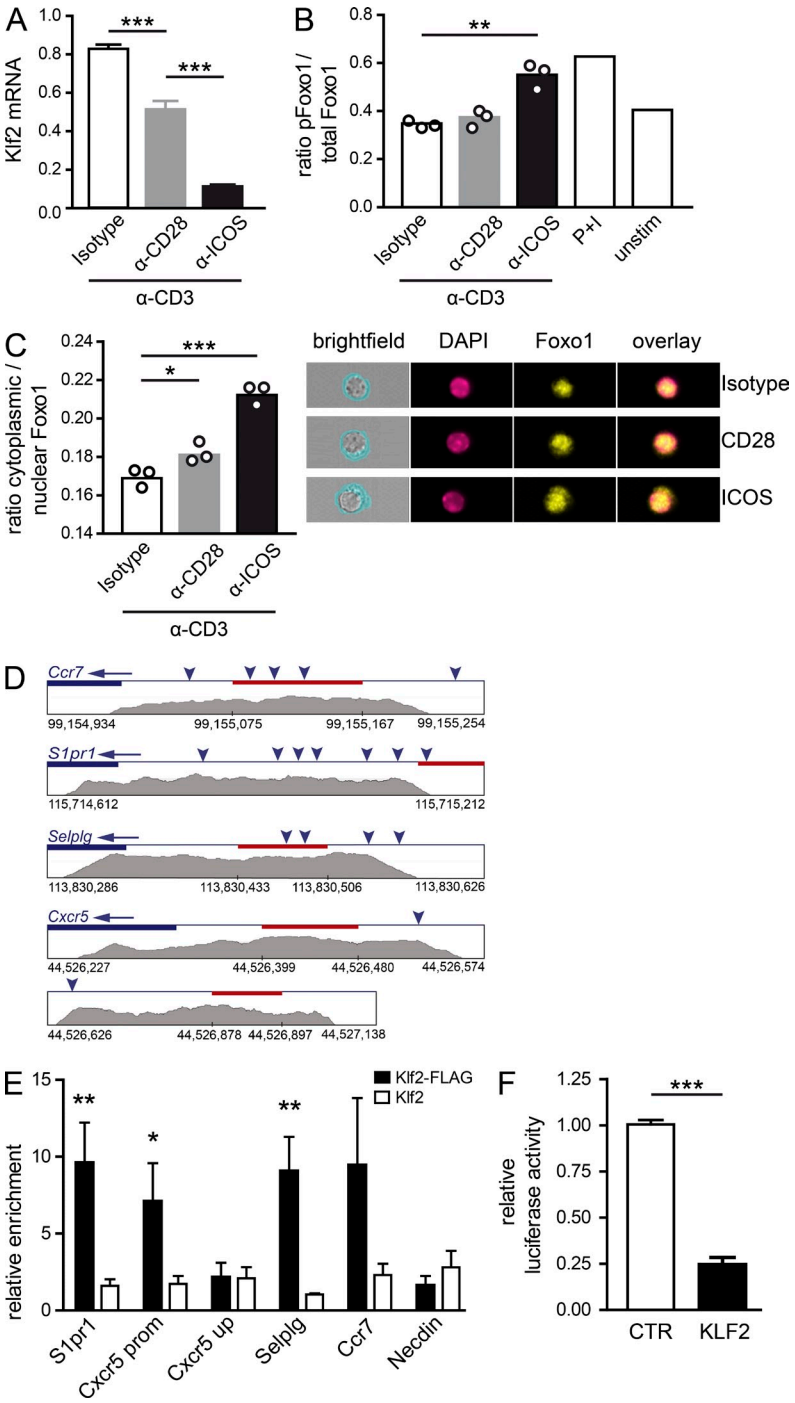

Figure 10. Klf2 is regulated via Foxo1 and directly binds to Cxcr5, Selplg, and Ccr7. (A–C) Naive CD4+ T cells were stimulated in vitro for 24 h with plate-bound antibodies against CD3 in combination with anti-CD28, anti-ICOS, or an isotype control. (A) *Klf2* mRNA was quantified by RT-PCR (expression relative to *Hprt*; mean ± SEM from triplicates and 4 independent experiments). (B) Foxo1 phosphorylation was analyzed by intracellular staining with antibodies against total Foxo1 and phosphorylated (Ser 265) Foxo1. As controls, cells were stimulated for 2 h with PMA and ionomycin or left unstimulated. (C) Nuclear/cytoplasmic translocation of Foxo1 was directly assessed by ImageStream flow cytometry. (D) Schematic representations of putative Klf2 binding sites (arrow heads) in the genes for *Ccr7*, *S1pr1*, *Selplg* (encoding PSGL-1), and *Cxcr5* (last two diagrams). Coding regions are in blue, PCR products are indicated by red lines. Genomic regions highly conserved between human and mouse (gray histograms showing the degree of conservation) were analyzed by rVista. (E) OT-II T cells were retrovirally transfected with *Klf2* containing or not containing a FLAG-tag. For both constructs, ChIP was performed with an anti-FLAG or an isotype control antibody. Putative Klf2-binding sites in the *S1pr1*, *Cxcr5*, *Selplg* (encoding PSGL-1), and *Ccr7* genes were analyzed by quantitative RT-PCR. Necdin, which has been shown to contain no Klf2-binding sites, served as a negative control. The enrichment of Klf2-binding sites was normalized against the isotype control and is shown in comparison to the non-FLAG construct. Pooled data from 4 independent experiments, mean enrichment ± SEM. (F) HEK cells were transfected with a luciferase expression plasmid containing the Klf2-binding site from the *Cxcr5* promotor in front of a SV40 minimal promotor together with a Klf2 expression plasmid or empty control plasmid. After 24 h, firefly luciferase activity (relative to renilla luciferase) was determined. Pooled data from two independent experiments, with quadruplicates. *, $P < 0.05$; **, $P < 0.01$; ***, $P < 0.001$.

of TFH differentiation, ICOS is important for the maintenance of the TFH phenotype.

Both co-stimulatory receptors share the ability to recruit PI3K and signal downstream via Akt. Although the general importance of PI3K for the GC reaction has been previously highlighted (Gigoux et al., 2009; Rolf et al., 2010; Xiao et al., 2014), the exact downstream signaling mechanisms for ICOS and CD28 regarding TFH cell differentiation have been unknown. In vitro studies suggested that ICOS signaling via c-Maf might be important for TFH cell development (Bauquet et al., 2009), and ICOS can clearly regulate c-Maf during Th2 cell differentiation (Nurieva et al., 2003). However, effects of ICOS co-stimulation on IL-4 production can only be observed in APC-free in vitro systems (Nurieva et al., 2003; Watanabe et al., 2005). Since we observed no ICOS-dependent regulation of c-Maf, ICOS co-stimulation for this

transcription factor might have been replaced by other pathways in our in vivo model.

Using a viral infection model for TFH cell differentiation, Choi et al. (2011) recently claimed that ICOS co-stimulation is required for early up-regulation of Bcl-6. Importantly, this study analyzed Bcl-6 in coexpression with CXCR5, only. Using our protein-based immunization system and the same method of CXCR5/Bcl-6 coexpression analysis, we are able to fully reproduce these results with a highly significant difference in CXCR5/Bcl-6 double-positive cells in ICOS KO compared with WT mice and reduced Bcl-6 levels of ICOS KO T cells compared with WT CXCR5^{high} T cells (unpublished data). However, our study shows that the primary defect in ICOS KO mice is the impaired up-regulation of CXCR5, not of Bcl-6. Further, we identified a novel Bcl-6–independent pathway of CXCR5 regulation in T cells via the transcriptional repressor Klf2.

We found that 20 h after ICOS-L blockade, CXCR5 and other TFH-related molecules were substantially reduced, whereas Bcl-6 protein remained unchanged at that time (Fig. 5). The recently described ICOS–osteopontin pathway (Leavenworth et al., 2015), which seems to act later on the TFH cell phenotype than the ICOS–Klf2 pathway, can explain the subsequent loss of Bcl-6 between 20 and 48 h of ICOS-L blockade.

Klf2 is a zinc-finger transcription factor that is widely expressed in various tissues (Hart et al., 2012). Klf2 is thought to have an important role in the migration of T cells by up-regulating S1PR1 and CD62L, two molecules important for the exit of T cells from the thymus (Carlson et al., 2006; Bai et al., 2007). Mice with a T cell–specific KO for Klf2 have increased numbers of T cells in the thymus and in nonlymphoid tissues, which might be explained by an increased expression of inflammatory chemokine receptors (Sebzda et al., 2008). Until now, Klf2 was only known as a factor regulating interorgan T cell migration, e.g., between thymus and secondary lymphoid organs or secondary lymphoid organs and peripheral tissues (Sinclair et al., 2008; Hart et al., 2012). Here, we show that Klf2 also plays a key role in intraorgan TFH cell migration. Low levels of Klf2 are required to keep the typical B cell zone homing receptor pattern, with high expression of CXCR5 and low expression of CCR7, CD62L, PSGL-1, and S1PR1. The increased S1PR1 expression after blocking ICOS-L did not result in lymph node exit but in a relocation of TFH cells from the B cell follicle to the T cell zone. Subsequently, TFH cells lose expression of their master transcription factor Bcl-6, which can be explained by osteopontin-dependent degradation of Bcl-6 protein (Leavenworth et al., 2015) or by missing contact to antigen-specific B cells (Kerfoot et al., 2011).

What could be the unique signal from B cells for TFH maintenance? One simple explanation would be T cell receptor triggering. At that stage of the immune response, only B cells still have the capability to present antigen due to their access to antigen depots on follicular dendritic cells, whereas DCs in the T cell zone, which originally presented the antigen, are already extinct (De Smedt et al., 1998; Deenick et al., 2010; Baumjohann et al., 2013; Weinstein et al., 2014). Previously, we demonstrated antigen dependence of fully matured TFH cells by transferring sorted TFH cells either into naive hosts or mice challenged with the cognate antigen. Upon transfer into mice challenged with cognate antigen, TFH cells retained their phenotype (Weber et al., 2012).

Why is CD28 co-stimulation no longer important for the maintenance of the TFH cell phenotype? First, we showed that CD28 is clearly inferior in regulating Klf2 compared with ICOS. This might be explained by the fact that ICOS preferentially recruits the p110/p50α isoform of PI3K, which is known to have a stronger lipid kinase activity than p110/p85α (Fos et al., 2008) and therefore has a higher potential to phosphorylate Foxo1, resulting in lower levels of Klf2. Second, the different expression patterns and hence availability of the ligands for CD28 and ICOS might explain the inverted roles in early and late phases of the immune responses. On B cells, expression of the CD28 ligands CD80 and CD86 is much lower compared with DC in the T cell zone (Lenschow et al., 1993), whereas ICOS-L is most highly expressed on B cells (Liang et al., 2002). Therefore, CD28 signaling might even be able to substitute for ICOS signaling in early T–DC interactions. This situation changes once the T cell is inside the B cell follicle, where ICOS gains importance compared with CD28. The more important role of ICOS during T/B compared with T/DC interaction is also emphasized by the fact that a B cell–specific KO of ICOS-L is sufficient to significantly reduce TFH cell frequencies (Nurieva et al., 2008; Pepper et al., 2011).

What does all of this mean for blocking ICOS and CD28 co-stimulation as a therapeutic option for the treatment of autoimmune diseases? The ability to block ICOS co-stimulation to act rapidly on already differentiated TFH cells is a clear advantage over CD28 blockade, which mainly prevents their de novo generation. With the specific effect on already differentiated effector T cells, blocking ICOS signaling does not further result in general immunosuppression. Thereby, blocking of ICOS co-stimulation is a promising new therapeutic approach to treat autoimmune diseases.

MATERIALS AND METHODS

Mice. Ovalbumin-specific TCR-transgenic OT-II mice (004194; JAX) on a WT, ICOS KO (Özkaynak et al., 2001), or CD28 KO (J002666; JAX) background were additionally crossed to B6PL mice (000406; JAX; Thy 1.1$^+$) to track cells in adoptive transfer experiments. For the inducible retroviral overexpression system, WT OT-II mice were crossed to Cre-ER^{T2} mice (Indra et al., 1999). NP-specific B cell receptor knock-in B1-8i mice (Sonoda et al., 1997) were crossed to kappa-light chain KO mice (Zou et al., 1993) to ensure NP-specificity of all B cells, and Ly-5.1 mice (002014; JAX; CD45.1$^+$) for tracking of transferred cells. Klf2 flox mice (Lee et al., 2006) were crossed to OT-II x CreER^{T2} mice. As recipient mice for adoptive transfer experiments, normal C57BL/6, CD28 KO, or CD80/CD86 double KO mice (003610; JAX) were used. All mice had been backcrossed for at least 10 generation to C57BL/6 and were bred under specific pathogen–free conditions in the animal facility of the Federal Institute for Risk Assessment (Berlin, Germany). Female mice were used for experiments at the age of 8–14 wk. Animal handling and

experiments were conducted according to the German animal protection laws and approved by the responsible governmental authority (LAGeSo).

Adoptive transfer experiments. 2.5×10^5 naive (magnetically sorted for $CD62L^{high}$) transgenic OT-II T cells were adoptively transferred by i.v. injection into C57BL/6 mice. For some experiments, 10^6 B1-8i B cells were co-transferred. 16–24 h later, recipient mice were injected subcutaneously at the tail base with 50 µg NP-OVA in complete Freund's adjuvant (Sigma-Aldrich). Draining inguinal lymph nodes were analyzed as indicated. Transgenic T cells were identified in flow cytometry as $CD4^+$ $B220^-$ $CD8^-$ Thy-1.1^+. Transgenic B cells were defined as $CD19^+$ $CD3^-$ $CD8^-$ Ly-6G/C^- $CD45.2^-$ $CD45.1^+$. To block the CD28 or ICOS pathways, 240 µg CTLA-4–Ig (Linsley et al., 1992) or 150 µg MIL-5733 (Frey et al., 2010; anti–ICOS-L) were injected i.p. twice on consecutive days. As controls, equal amounts of human Ig (Baxter) or a rat IgG2a isotype control (clone 1D10) were used. Reagents were tested to be free of endotoxin. To induce nuclear translocation of Cre-ER^{T2} recombinase, mice were injected i.p. with 1 mg tamoxifen (Sigma-Aldrich) dissolved in sunflower oil on two consecutive days. For induction of Cre-ER^{T2} recombinase in vitro, (Z)-4-hydroxy-tamoxifen (Sigma-Aldrich) was used at 3 µM final concentration.

Sorting of antigen-specific T cells. Sorting of transgenic T cells was performed as described recently (Weber et al., 2012). In brief, transgenic T cells from inguinal lymph nodes were first enriched by magnetic sorting using Thy-1.1 microbeads (Miltenyi Biotec), followed by sorting on an ARIA II flow sorter (BD) for $CD4^+$ $B220^-$ $CD8^-$ Thy-1.1^+ $CD44^{high}$. For sorting of TFH and non-TFH cells, CXCR5 and PD-1 were used as additional markers. For the retransfer experiment, TFH cells were sorted as $B220^-$ $CD8^-$ Thy-1.2^- $CXCR5^+$ PD-1^+.

Flow cytometry. Single-cell suspensions from lymph nodes were stained with different combinations of the following monoclonal antibodies conjugated to Biotin, FITC, PE, PerCP, PE-Cy7, Alexa Fluor 647, Alexa Fluor 700, APC-Cy7, Pacific Blue, Pacific Orange, Brilliant Violet 711, or Brilliant Violet 785: KT3 (anti-CD3), YTS 191.1 or RM4-5 (anti-CD4), 53–6.72 (anti-CD8), 6D5 (anti-CD19), IM7.8.1 (anti-CD44), A20 (anti-CD45.1), 104 (anti-CD45.2), RA3-6B2 (anti-B220), MEL-14 (anti-CD62L), H1.2F3 (anti-CD69), OX-7 (anti-Thy-1.1), HO13 or 53–2.1 (anti-Thy-1.2), 2PH1 (anti-PSGL-1), 2G8 (anti-CXCR5), 4B12 (anti-CCR7), J43 or 29F.1A12 (anti-PD-1), RB6-8C5 (anti-Ly-6G/C), GL7, and PNA (anti-CG B cells). Streptavidin-PE-Cy7 was used as secondary reagent for biotinylated antibodies. Fc-receptors were blocked with 2.4G2 (anti-CD16/32). Antibodies were purchased from BioLegend, eBioscience, and BD, or were purified from hybridoma supernatants and coupled to fluorophores by standard procedures. To detect early apoptotic cells, a FITC-conjugated inhibitor of caspase-3 (CaspGLOW; eBioscience) was used according to the manufacturer's instructions.

For intracellular staining, antibodies against Bcl-6 (GI191E/A8), CD40L (MR1), anti-pFoxo1 (Ser 256), and anti-Foxo1 (C29H4; Cell Signaling Technology; in combination with Alexa Fluor 647–conjugated anti–rabbit IgG) were used together with the FoxP3 Staining Buffer Set from eBioscience. For analysis of cytokine production, cells were restimulated in vitro with $OVA_{323-339}$ peptide for 2 h in the presence of Brefeldin A, fixed with paraformaldehyde, and permeabilized with saponin. Unspecific binding sites were blocked with 100 µg/ml 2.4G2 and 50 µg/ml purified rat Ig (Nordic) and cells were stained intracellularly with PE-Cy7–conjugated BVD6-24G2 (anti–IL-4) and an IL-21R-Fc chimeric protein (R&D Systems), followed by Alexa Fluor 647–conjugated anti–human Ig.

To discriminate dead cells, DAPI was added to live cells immediately before analysis or cells were stained on ice for 25 min with 1.34 µM Pacific Orange succinimidyl ester (Invitrogen) before fixation. Cells were analyzed on an LSR II, LSR Fortessa (BD), MACSQuant (Miltenyi Biotec), or an ImageStream^X Mark II (Amnis). Analysis gates were set on live cells defined by scatter characteristics and exclusion of DAPI- or Pacific Orange–positive cells. Data were further analyzed with FlowJo Software (Tree Star).

Histology. Lymph nodes were embedded in TissueTek OCT compound and 8 µm cryostat sections were prepared and fixed in acetone. After peroxidase inactivation and blocking of unspecific binding sites with Casein Solution (Vector Laboratories) supplemented with mAb 2.4G2 (100 µg/ml), sections were stained with FITC-coupled OX-7 (anti-Thy-1.1), Alexa Fluor 555–coupled RA3-6B2 (anti-B220), and Alexa Fluor 594–coupled GK1.5 (anti-CD4). Signals for Thy-1.1 were amplified with peroxidase-conjugated anti-FITC followed by Alexa Fluor 647–coupled tyramide (Invitrogen). Nuclei were stained with DAPI. Whole lymph node sections were captured on an LSM 780 with ZEN2010 imaging software using the tile-scan function (Carl Zeiss).

At least 6 sections from different areas of each lymph node were used for quantification of signals. For this purpose, total lymph node area (any signal) and B cell follicles ($B220^+$) were defined and transgenic T cell signal (Thy-1.1) was separated from background and unified by setting an appropriate threshold. Localization of T cells was determined by automatically counting pixels positive for the Thy-1.1 signal in the distinct lymph node compartments. Mean B cell follicle sizes were similar between groups.

ELISA for NP-specific IgG. Plates were coated with NP_3-BSA (Biosearch Technologies). Bound antibodies from sera were detected using HRP-coupled antibodies to mouse IgG1 or IgG2a (Southern Biotechnologies) and tetramethylbenzidine as substrate. As standard, NP-specific antibodies 18–1-16 (IgG1) and S43-10 (IgG2a; Reth et al., 1978) were used.

In vitro co-stimulation assays. High protein-binding capacity cell culture plates were coated with anti-CD3 (145-2C11, 5–15 ng/ml) and anti-CD28 (37.51), anti-ICOS (C398.4A), or a hamster isotype control. Purified naive $CD4^+$ T cells (magnetic depletion of $B220^+$ $CD11b^+$ $CD11c^+$ $NK1.1^+$ $CD8^+$ $CD44^+$ cells; Miltenyi Biotec) were incubated on plates for 24 h at 37°C, 5% CO_2.

Quantitative RT-PCR and gene expression profiling. For quantitative PCR, total RNA was isolated using the Roche High Pure RNA Isolation kit. RNA quality was checked on an Agilent Bioanalyzer and cDNA synthesized with the Applied Biosystems High Capacity cDNA kit. Gene expression was analyzed using primer/probe sets or primers in combination with SYBR Green on an Applied Biosystems 7500 Real Time PCR System. To standardize expression levels, β2-microglobulin or hypoxanthine-guanine phospho-ribosyltransferase (Hprt) as housekeeping genes were amplified.

The following Taqman assays from Applied Biosystems were used: hu Ascl2 (Hs00270888_s1), hu Bcl6 (Hs00153368_m1), hu Cxcr5 (Hs00173527_m1), hu Hprt (Hs02800695_m1), hu S1pr1 (Hs00173499_m1), hu Sell (Hs00174151_m1), mu Ascl2 (Mm01268891_g1), mu c-maf (Mm02581355_s1), mu Gata3 (Mm00484683_m1), mu Hprt (Mm01545399_m1), mu Klf2 (Mm01244979_g1), mu Prdm1 (Mm00476128_m1), mu S1pr1 (Mm00514644_m1), and mu Tbx21 (Mm00450960_m1). Additional primers used were as follows: hu Hprt (5′-GCTATAAATTCTTTGCTGACCTGCTG-3′ and 5′-AATTACTTTTATGTCCCCTGTTGACTGG-3′), hu Klf2 (5′-GCACGCACACAGGTGAGAAG-3′ and 5′-ATGTGCCGTTTCATGTGCAGC-3′), mu β2m (5′-ATTCACCCCCACTGAGACTGA-3′, 5′-CTCGATCCCAGTAGACGGTC-3′ and 5′-FAM-TGCAGAGTTAAGCATGCCAGTATGGCCG-TAMRA-3′).

For gene expression profiling, total RNA was isolated with the QIAGEN RNeasy purification kit. Labeling and hybridization of Affymetrix Mouse Genome 430 2.0 arrays was performed according to the manufacturer's instructions. Data were further analyzed using High Performance Chip Data Analysis (HPCDA) with BioRetis database as recently validated and described (Menssen et al., 2009). Original microarray data are available in the Gene Expression Omnibus database under the accession no. GSE49314.

Retroviral infection. For constitutive overexpression, the coding region of Klf2 was cloned into a modified version of the retroviral expression vector pMSCV (Takara Bio Inc.) which additionally encodes GFP via an IRES site.

For inducible overexpression, the vector pMSCV-loxp-dsRed-loxp-eGFP-Puro-WPRE (Koo et al., 2012), in which the eGFP cassette has been replaced by Klf2, was used. The coding region of Ascl2 was cloned into pMSCV with a human CD4 reporter instead of GFP. Viral particles were generated in HEK293 cells by calcium phosphate transfection using the packaging plasmids pECO and pCpG. In vitro prestimulated OT-II T cells ($OVA_{323-339}$ peptide for 36 h) were infected with retroviral supernatants by centrifugation for 90 min at 700× g, 32°C and 8 µg/ml polybrene. Residual virus was thoroughly washed away before the OT-II cells were used for subsequent studies. Infected cells were either directly transferred into recipient mice or cultured for additional 20 h in vitro to sort for fluorescent protein expressing cells on a FACSAria II flow sorter (BD).

ChIP. ChIP was performed as described previously (Stittrich et al., 2010) with retrovirally transduced T cells overexpressing either normal Klf2 or a FLAG-tagged version. In brief, 2×10^6 cells were fixed with 1% formaldehyde and chromatin was sheared to 200–800 bp of length by sonication. DNA was precipitated using 4 µg/ml monoclonal anti-FLAG antibody (clone M2; Sigma-Aldrich) or isotype control antibody (18–1-16) and measured by SYBR Green based RT-PCR for putative Klf2 binding sites. Primer pairs used were: Ccr7 (5′-GGCAGGGAGGAAGTGGTAAGAG-3′ and 5′-CCTTGTGGCCCAGGAAGACT-3′), Cxcr5 prom (5′-AGGCTGGTCACTGTCTGATGTC-3′ and 5′-TGTTTAAGTTTGCAGCTGACGCC-3′), Cxcr5 up (5′-CCAGTTTGCCCAGAACCAAAGAAAGTC-3′ and 5′-GCAAAAGGATGGCAGTCACAGG-3′), Necdin (5′-TTCGTCCAGCAGAATTACCTGAAG-3′ and 5′-GGACCCCCAGAAGAACTCGTA-3′), S1pr1 (5′-GCCTGGCAGCTCCTAAATTCTAA-3′ and 5′-ATCCCCATGCCTAGTTTCAGAGT-3′), and Selplg (5′-CCAGACACTTGTGGTCCCAAT-3′, 5′-CCTCATTCTCGCTTCCTTCTTC-3′). Fold enrichment was calculated as $2\text{^}(Ct_{input} - Ct_{test})$ and expressed relative to the IgG control. Putative binding sites for Klf2 (CACCC and GC-Box binding motifs such as for SP1 and MZF1) in mouse/human conserved regions of the Selplg, Cxcr5, Ccr7, and S1pr1 locus were identified with the web server of the comparative tool rVista based on the professional V10.2 library of the TRANSFAC database (matrix similarity predefined as 0.75). Necdin was used as a negative control for Klf2 binding, as previously described (Alhashem et al., 2011).

Luciferase reporter assay. The identified KLF2-binding site in the Cxcr5 promotor (GAGGCAAGCA) was cloned into the pGL3 minimal promotor luciferase plasmid (Promega). HEK cells were cotransfected with pGL3, pcDNA3-Klf2, and pRL-TK Renilla luciferase plasmid by calcium phosphate precipitation. Luciferase activity was measured on an Orion L Microplate Luminometer (Berthold) after 24 h using the dual luciferase assay system (Promega). Data were normalized to the activity of Renilla luciferase.

Analysis of human TFH cells. Human tonsils from patients undergoing routine tonsillectomy were obtained after informed consent and in accordance with the local ethics committee of the Charité University Medicine Berlin. Mononuclear cells were prepared by mechanical disruption of tissue and ficoll density centrifugation. The following monoclonal antibodies conjugated to Biotin, FITC, PE, Alexa Fluor 647, Alexa Fluor 700, or Pacific Blue were used for flow cytometry staining: OKT3 (anti-CD3), 91d6 (anti-CD4), 1H3 (anti-CD62L), FN50 (anti-CD69), KPL-1 (anti-PSGL-1), 3D12 (anti-CCR7), RF8B2 (anti-CXCR5), and F44 (anti-ICOS; Hutloff et al., 1999). For functional assays, tonsillar cells were cultured in round bottom tubes in RPMI 1640 in the presence of 20 pg/ml staphylococcal enterotoxin B (Toxin Technology) and either 20 µg/ml blocking anti–ICOS-L antibody HIL-131 (Khayyamian et al., 2002) or a murine IgG1 isotype control (18–1-16). To ensure immediate T/B contact, cells were centrifuged at 50× g for 5 min.

Experimental design, data presentation, and statistical analysis. Experimental groups consisted of 5 to 8 individual mice per group (randomly assigned) which routinely provides the statistical power to detect biological significant differences in our experimental system. For RNA isolation, cells from at least 15 animals were pooled. Data are presented either showing the mean and results from single animals, or the mean with error bars (standard error of mean). No data exclusion criteria were used. Data were analyzed using GraphPad Prism 5. Differences between the means of groups were calculated using unpaired, two-tailed Student's *t* tests.

We thank Heidi Schliemann, Monika Jaensch, Petra Jahn, and Ewa Schlereth for expert technical assistance, Fabian Kriegel for help with the quantification algorithm for histology, Matthias Pink and Christian Neumann for help with the luciferase assay, and Claudia Giesecke for provision of additional tonsil samples. Klaus Rajewsky kindly provided B1-8i mice.

This work was supported by DFG grants HU 1294/1-2 and HU 1294/4-1 to A. Hutloff, ERC Advanced Grant 268987 to A. Radbruch, and the e:Bio program of the Federal Ministry of Education to M.-F. Mashregi.

The authors declare no competing financial interests.

Submitted: 29 July 2014
Accepted: 16 January 2015

REFERENCES

Akiba, H., K. Takeda, Y. Kojima, Y. Usui, N. Harada, T. Yamazaki, J. Ma, K. Tezuka, H. Yagita, and K. Okumura. 2005. The role of ICOS in the CXCR5+ follicular B helper T cell maintenance in vivo. *J. Immunol.* 175:2340–2348. http://dx.doi.org/10.4049/jimmunol.175.4.2340

Alhashem, Y.N., D.S. Vinjamur, M. Basu, U. Klingmüller, K.M. Gaensler, and J.A. Lloyd. 2011. Transcription factors KLF1 and KLF2 positively regulate embryonic and fetal beta-globin genes through direct promoter binding. *J. Biol. Chem.* 286:24819–24827. http://dx.doi.org/10.1074/jbc.M111.247536

Bai, A., H. Hu, M. Yeung, and J. Chen. 2007. Kruppel-like factor 2 controls T cell trafficking by activating L-selectin (CD62L) and sphingosine-1-phosphate receptor 1 transcription. *J. Immunol.* 178:7632–7639. http://dx.doi.org/10.4049/jimmunol.178.12.7632

Baumjohann, D., S. Preite, A. Reboldi, F. Ronchi, K.M. Ansel, A. Lanzavecchia, and F. Sallusto. 2013. Persistent antigen and germinal center B cells sustain T follicular helper cell responses and phenotype. *Immunity.* 38:596–605. http://dx.doi.org/10.1016/j.immuni.2012.11.020

Bauquet, A.T., H. Jin, A.M. Paterson, M. Mitsdoerffer, I.C. Ho, A.H. Sharpe, and V.K. Kuchroo. 2009. The costimulatory molecule ICOS regulates the expression of c-Maf and IL-21 in the development of follicular T helper cells and TH-17 cells. *Nat. Immunol.* 10:167–175. http://dx.doi.org/10.1038/ni.1690

Bossaller, L., J. Burger, R. Draeger, B. Grimbacher, R. Knoth, A. Plebani, A. Durandy, U. Baumann, M. Schlesier, A.A. Welcher, et al. 2006. ICOS deficiency is associated with a severe reduction of CXCR5+CD4 germinal center Th cells. *J. Immunol.* 177:4927–4932. http://dx.doi.org/10.4049/jimmunol.177.7.4927

Carlson, C.M., B.T. Endrizzi, J. Wu, X. Ding, M.A. Weinreich, E.R. Walsh, M.A. Wani, J.B. Lingrel, K.A. Hogquist, and S.C. Jameson. 2006. Kruppel-like factor 2 regulates thymocyte and T-cell migration. *Nature.* 442:299–302. http://dx.doi.org/10.1038/nature04882

Choi, Y.S., R. Kageyama, D. Eto, T.C. Escobar, R.J. Johnston, L. Monticelli, C. Lao, and S. Crotty. 2011. ICOS receptor instructs T follicular helper cell versus effector cell differentiation via induction of the transcriptional repressor Bcl6. *Immunity.* 34:932–946. http://dx.doi.org/10.1016/j.immuni.2011.03.023

Craft, J.E. 2012. Follicular helper T cells in immunity and systemic autoimmunity. *Nat Rev Rheumatol.* 8:337–347. http://dx.doi.org/10.1038/nrrheum.2012.58

Crotty, S. 2011. Follicular helper CD4 T cells (TFH). *Annu. Rev. Immunol.* 29:621–663. http://dx.doi.org/10.1146/annurev-immunol-031210-101400

De Smedt, T., B. Pajak, G.G. Klaus, R.J. Noelle, J. Urbain, O. Leo, and M. Moser. 1998. Antigen-specific T lymphocytes regulate lipopolysaccharide-induced apoptosis of dendritic cells in vivo. *J. Immunol.* 161:4476–4479.

Deenick, E.K., A. Chan, C.S. Ma, D. Gatto, P.L. Schwartzberg, R. Brink, and S.G. Tangye. 2010. Follicular helper T cell differentiation requires continuous antigen presentation that is independent of unique B cell signaling. *Immunity*. 33:241–253. http://dx.doi.org/10.1016/j.immuni.2010.07.015

Fabre, S., F. Carrette, J. Chen, V. Lang, M. Semichon, C. Denoyelle, V. Lazar, N. Cagnard, A. Dubart-Kupperschmitt, M. Mangeney, et al. 2008. FOXO1 regulates L-Selectin and a network of human T cell homing molecules downstream of phosphatidylinositol 3-kinase. *J. Immunol*. 181:2980–2989. http://dx.doi.org/10.4049/jimmunol.181.5.2980

Fos, C., A. Salles, V. Lang, F. Carrette, S. Audebert, S. Pastor, M. Ghiotto, D. Olive, G. Bismuth, and J.A. Nunès. 2008. ICOS ligation recruits the p50alpha PI3K regulatory subunit to the immunological synapse. *J. Immunol*. 181:1969–1977. http://dx.doi.org/10.4049/jimmunol.181.3.1969

Frey, O., J. Meisel, A. Hutloff, K. Bonhagen, L. Bruns, R.A. Kroczek, L. Morawietz, and T. Kamradt. 2010. Inducible costimulator (ICOS) blockade inhibits accumulation of polyfunctional T helper 1/T helper 17 cells and mitigates autoimmune arthritis. *Ann. Rheum. Dis*. 69:1495–1501. http://dx.doi.org/10.1136/ard.2009.119164

Gigoux, M., J. Shang, Y. Pak, M. Xu, J. Choe, T.W. Mak, and W.K. Suh. 2009. Inducible costimulator promotes helper T-cell differentiation through phosphoinositide 3-kinase. *Proc. Natl. Acad. Sci. USA*. 106:20371–20376. http://dx.doi.org/10.1073/pnas.0911573106

Grimbacher, B., A. Hutloff, M. Schlesier, E. Glocker, K. Warnatz, R. Dräger, H. Eibel, B. Fischer, A.A. Schäffer, H.W. Mages, et al. 2003. Homozygous loss of ICOS is associated with adult-onset common variable immunodeficiency. *Nat. Immunol*. 4:261–268. http://dx.doi.org/10.1038/ni902

Hart, G.T., K.A. Hogquist, and S.C. Jameson. 2012. Krüppel-like factors in lymphocyte biology. *J. Immunol*. 188:521–526. http://dx.doi.org/10.4049/jimmunol.1101530

Haynes, N.M., C.D. Allen, R. Lesley, K.M. Ansel, N. Killeen, and J.G. Cyster. 2007. Role of CXCR5 and CCR7 in follicular Th cell positioning and appearance of a programmed cell death gene-1high germinal center-associated subpopulation. *J. Immunol*. 179:5099–5108. http://dx.doi.org/10.4049/jimmunol.179.8.5099

Hedrick, S.M., R. Hess Michelini, A.L. Doedens, A.W. Goldrath, and E.L. Stone. 2012. FOXO transcription factors throughout T cell biology. *Nat. Rev. Immunol*. 12:649–661. http://dx.doi.org/10.1038/nri3278

Hutloff, A., A.M. Dittrich, K.C. Beier, B. Eljaschewitsch, R. Kraft, I. Anagnostopoulos, and R.A. Kroczek. 1999. ICOS is an inducible T-cell co-stimulator structurally and functionally related to CD28. *Nature*. 397:263–266. http://dx.doi.org/10.1038/16717

Indra, A.K., X. Warot, J. Brocard, J.M. Bornert, J.H. Xiao, P. Chambon, and D. Metzger. 1999. Temporally-controlled site-specific mutagenesis in the basal layer of the epidermis: comparison of the recombinase activity of the tamoxifen-inducible Cre-ER(T) and Cre-ER(T2) recombinases. *Nucleic Acids Res*. 27:4324–4327. http://dx.doi.org/10.1093/nar/27.22.4324

Kerdiles, Y.M., D.R. Beisner, R. Tinoco, A.S. Dejean, D.H. Castrillon, R.A. DePinho, and S.M. Hedrick. 2009. Foxo1 links homing and survival of naive T cells by regulating L-selectin, CCR7 and interleukin 7 receptor. *Nat. Immunol*. 10:176–184. http://dx.doi.org/10.1038/ni.1689

Kerfoot, S.M., G. Yaari, J.R. Patel, K.L. Johnson, D.G. Gonzalez, S.H. Kleinstein, and A.M. Haberman. 2011. Germinal center B cell and T follicular helper cell development initiates in the interfollicular zone. *Immunity*. 34:947–960. http://dx.doi.org/10.1016/j.immuni.2011.03.024

Khayyamian, S., A. Hutloff, K. Büchner, M. Gräfe, V. Henn, R.A. Kroczek, and H.W. Mages. 2002. ICOS-ligand, expressed on human endothelial cells, costimulates Th1 and Th2 cytokine secretion by memory CD4+ T cells. *Proc. Natl. Acad. Sci. USA*. 99:6198–6203. http://dx.doi.org/10.1073/pnas.092576699

Koo, B.K., D.E. Stange, T. Sato, W. Karthaus, H.F. Farin, M. Huch, J.H. van Es, and H. Clevers. 2012. Controlled gene expression in primary Lgr5 organoid cultures. *Nat. Methods*. 9:81–83. http://dx.doi.org/10.1038/nmeth.1802

Leavenworth, J.W., B. Verbinnen, J. Yin, H. Huang, and H. Cantor. 2015. A p85α-osteopontin axis couples the receptor ICOS to sustained Bcl-6 expression by follicular helper and regulatory T cells. *Nat. Immunol*. 16:96–106. http://dx.doi.org/10.1038/ni.3050

Lee, J.S., Q. Yu, J.T. Shin, E. Sebzda, C. Bertozzi, M. Chen, P. Mericko, M. Stadtfeld, D. Zhou, L. Cheng, et al. 2006. Klf2 is an essential regulator of vascular hemodynamic forces in vivo. *Dev. Cell*. 11:845–857. http://dx.doi.org/10.1016/j.devcel.2006.09.006

Lenschow, D.J., G.H. Su, L.A. Zuckerman, N. Nabavi, C.L. Jellis, G.S. Gray, J. Miller, and J.A. Bluestone. 1993. Expression and functional significance of an additional ligand for CTLA-4. *Proc. Natl. Acad. Sci. USA*. 90:11054–11058. http://dx.doi.org/10.1073/pnas.90.23.11054

Liang, L., E.M. Porter, and W.C. Sha. 2002. Constitutive expression of the B7h ligand for inducible costimulator on naive B cells is extinguished after activation by distinct B cell receptor and interleukin 4 receptor-mediated pathways and can be rescued by CD40 signaling. *J. Exp. Med*. 196:97–108. http://dx.doi.org/10.1084/jem.20020298

Linsley, P.S., P.M. Wallace, J. Johnson, M.G. Gibson, J.L. Greene, J.A. Ledbetter, C. Singh, and M.A. Tepper. 1992. Immunosuppression in vivo by a soluble form of the CTLA-4 T cell activation molecule. *Science*. 257:792–795. http://dx.doi.org/10.1126/science.1496399

Linterman, M.A., R.J. Rigby, R. Wong, D. Silva, D. Withers, G. Anderson, N.K. Verma, R. Brink, A. Hutloff, C.C. Goodnow, and C.G. Vinuesa. 2009. Roquin differentiates the specialized functions of duplicated T cell costimulatory receptor genes CD28 and ICOS. *Immunity*. 30:228–241. http://dx.doi.org/10.1016/j.immuni.2008.12.015

Liu, X., X. Chen, B. Zhong, A. Wang, X. Wang, F. Chu, R.I. Nurieva, X. Yan, P. Chen, L.G. van der Flier, et al. 2014. Transcription factor achaete-scute homologue 2 initiates follicular T-helper-cell development. *Nature*. 507:513–518. http://dx.doi.org/10.1038/nature12910

McAdam, A.J., R.J. Greenwald, M.A. Levin, T. Chernova, N. Malenkovich, V. Ling, G.J. Freeman, and A.H. Sharpe. 2001. ICOS is critical for CD40-mediated antibody class switching. *Nature*. 409:102–105. http://dx.doi.org/10.1038/35051107

McHeyzer-Williams, M., S. Okitsu, N. Wang, and L. McHeyzer-Williams. 2012. Molecular programming of B cell memory. *Nat. Rev. Immunol*. 12:24–34. http://dx.doi.org/10.1038/nn3128

Menssen, A., G. Edinger, J.R. Grün, U. Haase, R. Baumgrass, A. Grützkau, A. Radbruch, G.R. Burmester, and T. Häupl. 2009. SiPaGene: A new repository for instant online retrieval, sharing and meta-analyses of GeneChip expression data. *BMC Genomics*. 10:98. http://dx.doi.org/10.1186/1471-2164-10-98

Nurieva, R.I., J. Duong, H. Kishikawa, U. Dianzani, J.M. Rojo, I. Ho, R.A. Flavell, and C. Dong. 2003. Transcriptional regulation of th2 differentiation by inducible costimulator. *Immunity*. 18:801–811. http://dx.doi.org/10.1016/S1074-7613(03)00144-4

Nurieva, R.I., Y. Chung, D. Hwang, X.O. Yang, H.S. Kang, L. Ma, Y.H. Wang, S.S. Watowich, A.M. Jetten, Q. Tian, and C. Dong. 2008. Generation of T follicular helper cells is mediated by interleukin-21 but independent of T helper 1, 2, or 17 cell lineages. *Immunity*. 29:138–149. http://dx.doi.org/10.1016/j.immuni.2008.05.009

Özkaynak, E., W. Gao, N. Shemmeri, C. Wang, J.C. Gutierrez-Ramos, J. Amaral, S. Qin, J.B. Rottman, A.J. Coyle, and W.W. Hancock. 2001. Importance of ICOS-B7RP-1 costimulation in acute and chronic allograft rejection. *Nat. Immunol*. 2:591–596. http://dx.doi.org/10.1038/89731

Pepper, M., A.J. Pagán, B.Z. Igyártó, J.J. Taylor, and M.K. Jenkins. 2011. Opposing signals from the Bcl6 transcription factor and the interleukin-2 receptor generate T helper 1 central and effector memory cells. *Immunity*. 35:583–595. http://dx.doi.org/10.1016/j.immuni.2011.09.009

Platt, A.M., V.B. Gibson, A. Patakas, R.A. Benson, S.G. Nadler, J.M. Brewer, I.B. McInnes, and P. Garside. 2010. Abatacept limits breach of self-tolerance in a murine model of arthritis via effects on the generation of T follicular helper cells. *J. Immunol*. 185:1558–1567. http://dx.doi.org/10.4049/jimmunol.1001311

Poholek, A.C., K. Hansen, S.G. Hernandez, D. Eto, A. Chandele, J.S. Weinstein, X. Dong, J.M. Odegard, S.M. Kaech, A.L. Dent, et al. 2010. In vivo regulation of Bcl6 and T follicular helper cell development. *J. Immunol*. 185:313–326. http://dx.doi.org/10.4049/jimmunol.0904023

Reth, M., G.J. Hämmerling, and K. Rajewsky. 1978. Analysis of the repertoire of anti-NP antibodies in C57BL/6 mice by cell fusion. I. Characterization

of antibody families in the primary and hyperimmune response. *Eur. J. Immunol.* 8:393–400. http://dx.doi.org/10.1002/eji.1830080605

Rolf, J., S.E. Bell, D. Kovesdi, M.L. Janas, D.R. Soond, L.M. Webb, S. Santinelli, T. Saunders, B. Hebeis, N. Killeen, et al. 2010. Phosphoinositide 3-kinase activity in T cells regulates the magnitude of the germinal center reaction. *J. Immunol.* 185:4042–4052. http://dx.doi.org/10.4049/jimmunol.1001730

Sebzda, E., Z. Zou, J.S. Lee, T. Wang, and M.L. Kahn. 2008. Transcription factor KLF2 regulates the migration of naive T cells by restricting chemokine receptor expression patterns. *Nat. Immunol.* 9:292–300. http://dx.doi.org/10.1038/ni1565

Shiow, L.R., D.B. Rosen, N. Brdicková, Y. Xu, J. An, L.L. Lanier, J.G. Cyster, and M. Matloubian. 2006. CD69 acts downstream of interferon-alpha/beta to inhibit S1P1 and lymphocyte egress from lymphoid organs. *Nature.* 440:540–544. http://dx.doi.org/10.1038/nature04606

Sinclair, L.V., D. Finlay, C. Feijoo, G.H. Cornish, A. Gray, A. Ager, K. Okkenhaug, T.J. Hagenbeek, H. Spits, and D.A. Cantrell. 2008. Phosphatidylinositol-3-OH kinase and nutrient-sensing mTOR pathways control T lymphocyte trafficking. *Nat. Immunol.* 9:513–521. http://dx.doi.org/10.1038/ni.1603

Sonoda, E., Y. Pewzner-Jung, S. Schwers, S. Taki, S. Jung, D. Eilat, and K. Rajewsky. 1997. B cell development under the condition of allelic inclusion. *Immunity.* 6:225–233. http://dx.doi.org/10.1016/S1074-7613(00)80325-8

Stittrich, A.B., C. Haftmann, E. Sgouroudis, A.A. Kühl, A.N. Hegazy, I. Panse, R. Riedel, M. Flossdorf, J. Dong, F. Fuhrmann, et al. 2010. The microRNA miR-182 is induced by IL-2 and promotes clonal expansion of activated helper T lymphocytes. *Nat. Immunol.* 11:1057–1062. http://dx.doi.org/10.1038/ni.1945

Tafuri, A., A. Shahinian, F. Bladt, S.K. Yoshinaga, M. Jordana, A. Wakeham, L.M. Boucher, D. Bouchard, V.S. Chan, G. Duncan, et al. 2001. ICOS is essential for effective T-helper-cell responses. *Nature.* 409:105–109. http://dx.doi.org/10.1038/35051113

Tangye, S.G., C.S. Ma, R. Brink, and E.K. Deenick. 2013. The good, the bad and the ugly - TFH cells in human health and disease. *Nat. Rev. Immunol.* 13:412–426. http://dx.doi.org/10.1038/nri3447

Tellier, J., and S.L. Nutt. 2013. The unique features of follicular T cell subsets. *Cell. Mol. Life Sci.* 70:4771–4784. http://dx.doi.org/10.1007/s00018-013-1420-3

Veerman, K.M., M.J. Williams, K. Uchimura, M.S. Singer, J.S. Merzaban, S. Naus, D.A. Carlow, P. Owen, J. Rivera-Nieves, S.D. Rosen, and H.J. Ziltener. 2007. Interaction of the selectin ligand PSGL-1 with chemokines CCL21 and CCL19 facilitates efficient homing of T cells to secondary lymphoid organs. *Nat. Immunol.* 8:532–539. http://dx.doi.org/10.1038/ni1456

Walker, L.S., A. Gulbranson-Judge, S. Flynn, T. Brocker, C. Raykundalia, M. Goodall, R. Förster, M. Lipp, and P. Lane. 1999. Compromised OX40 function in CD28-deficient mice is linked with failure to develop CXC chemokine receptor 5-positive CD4 cells and germinal centers. *J. Exp. Med.* 190:1115–1122. http://dx.doi.org/10.1084/jem.190.8.1115

Watanabe, M., S. Watanabe, Y. Hara, Y. Harada, M. Kubo, K. Tanabe, H. Toma, and R. Abe. 2005. ICOS-mediated costimulation on Th2 differentiation is achieved by the enhancement of IL-4 receptor-mediated signaling. *J. Immunol.* 174:1989–1996. http://dx.doi.org/10.4049/jimmunol.174.4.1989

Weber, J.P., F. Fuhrmann, and A. Hutloff. 2012. T-follicular helper cells survive as long-term memory cells. *Eur. J. Immunol.* 42:1981–1988. http://dx.doi.org/10.1002/eji.201242540

Weinstein, J.S., S.A. Bertino, S.G. Hernandez, A.C. Poholek, T.B. Teplitzky, H.N. Nowyhed, and J. Craft. 2014. B cells in T follicular helper cell development and function: separable roles in delivery of ICOS ligand and antigen. *J. Immunol.* 192:3166–3179. http://dx.doi.org/10.4049/jimmunol.1302617

Xiao, N., D. Eto, C. Elly, G. Peng, S. Crotty, and Y.C. Liu. 2014. The E3 ubiquitin ligase Itch is required for the differentiation of follicular helper T cells. *Nat. Immunol.* 15:657–666. http://dx.doi.org/10.1038/ni.2912

Xu, H., X. Li, D. Liu, J. Li, X. Zhang, X. Chen, S. Hou, L. Peng, C. Xu, W. Liu, et al. 2013. Follicular T-helper cell recruitment governed by bystander B cells and ICOS-driven motility. *Nature.* 496:523–527. http://dx.doi.org/10.1038/nature12058

Yao, S., Y. Zhu, and L. Chen. 2013. Advances in targeting cell surface signalling molecules for immune modulation. *Nat. Rev. Drug Discov.* 12:130–146. http://dx.doi.org/10.1038/nrd3877

Zou, Y.R., S. Takeda, and K. Rajewsky. 1993. Gene targeting in the Ig kappa locus: efficient generation of lambda chain-expressing B cells, independent of gene rearrangements in Ig kappa. *EMBO J.* 12:811–820.